NEUROSCIENCE
RESEARCH ARTICLE
A. N. Imber et al. / Neuroscience 381 (2018) 59–78

The Role of Ca^{2+} and BK Channels of Locus Coeruleus (LC) Neurons as a Brake to the CO_2 Chemosensitivity Response of Rats

Ann N. Imber,[a†] Luis G. A. Patrone,[b†] Ke-Yong Li,[a†] Luciane H. Gargaglioni[b*] and Robert W. Putnam[a‡]

[a] *Department of Neuroscience, Cell Biology and Physiology, Wright State University, Boonshoft School of Medicine, 3640 Colonel Glenn Highway, Dayton, OH 45435, USA*

[b] *Department of Animal Morphology and Physiology, Sao Paulo State University – UNESP/FCAV, Jaboticabal, SP, Brazil*

Abstract—The cellular mechanisms by which LC neurons respond to hypercapnia are usually attributed to an ''accelerator'' whereby hypercapnic acidosis causes an inhibition of K^+ channels or activation of Na^+ and Ca^{+2} channels to depolarize CO_2-sensitive neurons. Nevertheless, it is still unknown if this ''accelerator'' mechanism could be controlled by a brake phenomenon. Whole-cell patch clamping, fluorescence imaging microscopy and plethysmography were used to study the chemosensitive response of the LC neurons. Hypercapnic acidosis activates L-type Ca^{2+} channels and large conductance Ca-activated K^+ (BK) channels, which function as a ''brake'' on the chemosensitive response of LC neurons. Our findings indicate that both Ca^{2+} and BK currents develop over the first 2 weeks of postnatal life in rat LC slices and that this brake pathway may cause the developmental decrease in the chemosensitive firing rate response of LC neurons to hypercapnic acidosis. Inhibition of this brake by paxilline (BK channel inhibitor) returns the magnitude of the chemosensitive firing rate response from LC neurons in rats older than P10 to high values similar to those in LC neurons from younger rats. Inhibition of BK channels in LC neurons by bilateral injections of paxilline into the LC results in a significant increase in the hypercapnic ventilatory response of adult rats. Our findings indicate that a BK channel-based braking system helps to determine the chemosensitive respiratory drive of LC neurons and contributes to the hypercapnic ventilatory response. Perhaps, abnormalities of this braking system could result in hypercapnia-induced respiratory disorders and panic responses.

Key words: central control of breathing, neuronal acid sensing, panic disorder, paxilline, development.

INTRODUCTION

Chemosensitive neurons have been reported in many regions of the brain, including the amygdala (Ziemann et al., 2009), the locus coeruleus (LC) (Pineda and Aghajanian, 1997; Filosa and Putnam, 2003), the medullary raphe (Richerson, 1995; Wang et al., 1998), the nucleus tractus solitarius (NTS) (Dean et al., 1989; Conrad et al., 2009; Nichols et al., 2009), lateral hypothalamus (Williams et al., 2007) and the retrotrapezoid nucleus (RTN) (Mulkey et al., 2004; Ritucci et al., 2005a). The magnitude of the firing rate response of a neuron to a given acid stimulus can be expressed as the chemosensitivity index (CI), which represents a percentage increase in control neuronal firing rate per 0.2 pH unit decrease in external pH (pH_o) (Wang et al., 1998; Wang and Richerson, 1999). Neurons from different chemosensitive regions have widely different magnitudes of firing rate responses to hypercapnic acidosis, based on their CI, ranging from large responses (300%) in RTN neurons (Mulkey et al., 2004; Ritucci et al., 2005a) to very small responses (~125%, with 100% indicating a non-chemosensitive neuron) in LC neurons (Putnam et al., 2004; Gargaglioni et al., 2010).

The magnitude of the chemosensitive response is significant because a high degree of chemosensitivity

*Corresponding author. Address: Via de acesso Paulo Donato Castellane s/n, 14870-000, Departamento de Morfologia e Fisiologia Animal, Faculdade de Ciências Agrárias e Veterinárias, Universidade Estadual Paulista Júlio de Mesquita Filho, Jaboticabal, SP, Brazil.
E-mail address: lucihel@fcav.unesp.br (L. H. Gargaglioni).

† All three authors contributed equally to the work.

‡ Deceased.

Abbreviations: aCSF, artificial cerebral spinal fluid; BAPTA, cell permeant chelator; BK, large-conductance K_{Ca} channels; CI, chemosensitivity index; C_m, capacitance; CNS, central nervous system; CO_2, carbon dioxide; EGTA, ethylene glycol tetraacetic acid; FR, firing rate; f_R, respiratory frequency; HCO_3^-, bicarbonate; HEPES, 4-(2-hydroxyethyl)-1-piperazineethanesulfonic acid; HR, heart rate; K_{Ca}, potassium channel activated by intracellular calcium; LC, locus coeruleus; MAP, mean arterial pressure; NTS, nucleus tractus solitarius; O_2, oxygen; P, postnatal day; PAP, pulsatile arterial pressure; P_{CO2}, arterial carbon dioxide partial pressure; pH, hydrogen ion concentration; pHa, arterial pH; P_{O2}, arterial oxygen partial pressure; RTN, retrotrapezoid nucleus; S_k, small conductance; Tb, body temperature; TRP, transient receptor potential; TTX, tetrodotoxina; V_E, pulmonary ventilation; V_m, membrane potential; V_T, tidal volume.

https://doi.org/10.1016/j.neuroscience.2018.03.031
0306-4522/

has been correlated with several pathological conditions. Increased chemosensitivity has been observed in cases of sleep apnea (Verbraecken et al., 1995; Younes et al., 2001) and patients who experience periodic breathing during sleep (Chapman et al., 1988). Patients with panic disorder show an increased hypercapnic ventilatory response (Papp et al., 1993; Nardi et al., 2009), and several anti-anxiolytic drugs reduce the ventilatory response to hypercapnic acidosis (Pols et al., 1993; Gorman et al., 1997). Thus, understanding the cellular basis for the magnitude of the response of neurons to hypercapnic acidosis is likely to be of significance to human pathology.

Studies of the magnitude of the chemosensitive response of medullary and pontine neurons from neonatal animals are complicated by various developmental changes. For example, neurons from the NTS exhibit virtually no developmental changes either in the percentage of neurons that respond to hypercapnic acidosis or in the magnitude of that response (Conrad et al., 2009; Nichols et al., 2009). In contrast, neurons from the medullary raphé show a large increase in the magnitude of their response to hypercapnic acidosis after age postnatal day 12 (P12) (Hodges and Richerson, 2010). A completely different pattern is exhibited by LC neurons, with a marked decrease in the magnitude of the chemosensitive response to hypercapnic acidosis in LC neurons from rats aged >P10 (Gargaglioni et al., 2010). These differing developmental changes offer an interesting system for studying the cellular basis of the magnitude of the chemosensitive response.

The cellular basis for the firing rate response to hypercapnic acidosis in these chemosensitive neurons is not fully understood. Current studies have focused on many acid-sensitive ion channels from various regions of the brainstem including the LC, Raphe and RTN in rats, such as inwardly rectifying K^+ (K_{ir}) channels (Pineda and Aghajanian, 1997), delayed-rectifying K^+ (K_{dr}) channels (Denton et al., 2007; Putnam, 2010), transient K^+ channels (A current) (Denton et al., 2007; Putnam, 2010; Li and Putnam, 2013), TWIK-related acid-sensitive K^+ (TASK) channels (Bayliss et al., 2001), a calcium-activated non-selective cation (CAN) current (Putnam, 2010), acid-sensitive non-selective cation (ASIC) channels (Ziemann et al., 2009), transient receptor potential (TRP) channels (Cui et al., 2011), and L-type Ca^{2+} channels (Filosa and Putnam, 2003; Imber and Putnam, 2012; Imber et al., 2014). These channels are either inhibited (K_{ir}, K_{dr}, A current, and TASK) or activated (ASIC, CAN, TRP and L-type Ca^{2+} channels) by hypercapnic acidosis and this results in neuronal depolarization and increased neuron firing rate (Putnam et al., 2004; Putnam, 2010). Since these channels all result in increased neuronal firing rate in response to hypercapnic acidosis, they can be thought of as ‘‘accelerators” in the neuronal chemosensitive response.

The activation of Ca^{2+} channels by hypercapnic acidosis could be part of the accelerator pathway. Alternatively, we hypothesize that Ca^{2+} channels can work to decrease the chemosensitive response to hypercapnic acidosis. Ca^{2+} channel activation results in increased $[Ca^{2+}]_I$ (Imber and Putnam, 2012; Imber et al., 2014) and therefore could activate Ca^{2+}-activated K^+ (K_{Ca}) channels. This would lead to a hypercapnic acidosis-induced membrane hyperpolarization that could be thought of as a ‘‘brake” to the neuronal chemosensitive response.

To study the possible presence of a braking phenomenon we have chosen to use LC neurons. These neurons have been shown to be involved in both respiratory control (Biancardi et al., 2008) and the expression of anxiety and panic disorders (Bailey et al., 2003). Previous studies have confirmed the presence of large-conductance K_{Ca} channels (‘‘Big” K or BK channels) in the LC (Sausbier et al., 2006). Further, based on membrane potential (V_m) oscillations that arise from the activity of Ca^{2+} channels, Ca^{2+} channels are clearly present in LC neurons as well (Imber and Putnam, 2012). These Ca^{2+} channels show a developmental response in LC neurons, with higher Ca^{2+} channel activity after the age of P10 (Imber and Putnam, 2012). Interestingly, inhibition of Ca^{2+} channels reduces the firing rate response to hypercapnic acidosis in LC neurons from neonatal rats younger than P10 (Filosa and Putnam, 2003), suggesting that these channels participate in the accelerator pathway in LC neurons from young neonates. However, recent work suggests that blocking the activation of Ca^{2+} channels by hypercapnia increases the firing rate response to hypercapnia in LC neurons from rats older than P10 (Imber et al., 2014). This leads us to further hypothesize that the proposed braking pathway develops during the neonatal period. Since the observed fall in the magnitude of the chemosensitive response in LC neurons occurs after day P10, we propose that Ca^{2+} channels, and perhaps BK channels, show a concurrent increase in LC neurons during the neonatal period.

The main purposes of the current study were to test that L-type Ca^{2+} channels in LC neurons increase their current density during the first two weeks of neonatal development, are activated by hypercapnia and increase intracellular Ca^{2+}. Further, we sought to test that BK channels are present in LC neurons, that they increase in current density during the first two weeks of neonatal development and that inhibition of BK channels results in an increased firing rate response of LC neurons to hypercapnic acidosis, providing evidence for the presence of a hypercapnia-induced braking pathway in LC neurons. Finally, we wanted to characterize the magnitude of the brake in response to different levels of hypercapnia and study whether inhibition of the brake in LC neurons was sufficient to increase the hypercapnic ventilatory response to inspired CO_2 in adult rats.

EXPERIMENTAL PROCEDURES

Ethical approval

All procedures at Wright State University in which animals were involved were reviewed and approved by the Wright State University Institutional Animal Care and Use Committee and are in agreement with standards set out in the National Institutes of Health Guide for Care and Use of Laboratory Animals. Wright State University is accredited by AAALAC and is covered by NIH

Assurance (No. A3632-01). All procedures at Sao Paulo State University involving the use of animals were done in compliance with the guidelines of the National Council of Control in Animal Experimentation (CONCEA-MCT-Brazil), and with the approval of the Faculty of Agricultural and Veterinary Sciences Animal Care and Use Committee (CEUA-FCAV-UNESP-Jaboticabal campus; Protocol: 023217/13).

Slice preparation

Neonatal (P3–P16) Sprague–Dawley rat pups (mixed sex) were anesthetized using high CO_2 or hypothermia and then rapidly decapitated as previously described (Filosa et al., 2002; Ritucci et al., 2005b). Removal of the brainstem and subsequent coronal brain slicing using a vibratome (Pelco Vibratome 1000) was carried out in ice-cold (4–6 °C) artificial cerebrospinal fluid (aCSF). Slices containing the LC region were then incubated in room temperature aCSF equilibrated with 5% CO_2/95% O_2 until use 1–4 h after slicing. During experiments, slices were superfused continuously by gravity flow (~4 mL/min) using solutions held at 35 °C.

Solutions

Unless otherwise specified, all brain slices were immersed in aCSF. This solution consisted of (in mM): 124 NaCl, 3 KCl, 1.3 $MgSO_4$, 26 $NaHCO_3$, 1.24 NaH_2PO_4, 10 glucose, and 2.4 $CaCl_2$ and was equilibrated with 5% CO_2/95% O_2, pH_o ~7.45 (at 35 °C). Hypercapnic solutions were identical except for equilibration with 15% CO_2/85% O_2, pH_o ~7.0, 10% CO_2/90% O_2, pH_o ~7.15 or 7.5% CO_2/92.5 O_2%, pH_o ~7.25. Based on the Henderson–Hasselbalch equation, these translate into P_{CO2} values in solution of 38.7 mm Hg (5% CO_2), 61.4 mm Hg (7.5% CO_2), 77.2 mm Hg (10% CO_2) and 109.1 mm Hg (15% CO_2). These percentages of CO_2 were chosen to maximize cellular effects of hypercapnic acidosis (Pineda and Aghajanian, 1997; Ritucci et al., 2005b) and present a broad range of hypercapnic acidotic stimulation. The change in pH (0.2 pH unit) and CO_2 (23 mm Hg) in aCSF equilibrated with 7.5% CO_2 are similar to the change in pH (0.14 pH unit) and CO_2 (15 mm Hg) in rats breathing 7% CO_2 (Table 1). The changes in pH (0.30 pH unit) and CO_2 (38 mm Hg) in aCSF equilibrated with 10% CO_2 are similar to the changes of pH (0.23 pH unit) and CO_2 (23 mm Hg) in anesthetized adult rats breathing 10% CO_2 to induce panic (Ziemann et al., 2009).

The whole-cell pipette solution for current-clamp studies consisted of (in mM): 130 K-gluconate, 0.4 EGTA, 1 $MgCl_2$, 0.3 Na_2GTP, 2 Na_2ATP, and 10 HEPES. The pipette solution pH was buffered to ~7.35 using KOH. For intracellular Ca^{2+} (Ca_i^{2+}) measurements, 250 μM Fura-2 was also added to the pipette solution. The pipette filling solution for voltage-clamp studies of the Ca^{2+} current consisted of (in mM): 130 CsCl, 10 EGTA, 1 $MgCl_2$, 0.3 GTP, 2 ATP, 10 HEPES, and 10 tetraethyl ammonium (TEA), buffered to pH ~7.45 using CsOH. For voltage-clamp studies of BK currents, the pipette solution was identical to those used for current-clamp studies.

Measurement of intracellular Ca^{2+}

The Ca^{2+}-sensitive dye Fura-2 (250 μM) was loaded into LC neurons using whole-cell patch pipettes. Fura-2-loaded neurons were excited by light from a 75 W xenon arc lamp alternately at 340 nm and 380 nm using a Sutter Lambda 10–2 filter wheel. Emitted fluorescence at 505 nm was directed to the Nikon multi-image port module and then to a GenIISys Image intensifier and a CCD camera. Subsequent fluorescence images were acquired using a Gateway 2000 E-3100 computer and collected/processed using the software MetaFluor 4.6r. Image acquisition could be achieved within ~2 s and was repeated every 15 s. Light was blocked between acquisitions to reduce photobleaching. The Fura-2 fluorescence was not calibrated and arbitrary fluorescence units were used instead to monitor increases or decreases in the ratio of fluorescence (R_{fl} = Fl_{340}/Fl_{380}), and thereby increases or decreases in intracellular Ca^{2+}.

Electrophysiological recordings

Whole-cell recordings were used throughout this study. Pipettes were made from thin-walled borosilicate glass (outer diameter 1.5 mm, inner diameter 1.12 mm) pulled to a tip resistance of ~5 MΩ. In a 300-μm thickness slice, LC neurons were visualized using an upright microscope (Nikon Eclipse 6600) with an ×60 water-immersion objective and subsequently patched via formation of a gigaohm seal with the cell membrane. Electrical signals from individual neurons were obtained with an Axopatch 200B amplifier, a Digidata 1440A A/D convert and pCLAMP 10.2 software (all from Molecular Devices). An Ag-AgCl electrode connected to the bath solution via a KCl-agar bridge served as the reference electrode. Data were filtered at 2 kHz, sampled at 10 kHz, and saved on a computer to be analyzed offline.

For current-clamp recording, criteria for healthy neurons were a stable resting V_m of −40 to −60 mV and a spontaneous firing rate of < 4 Hz. Firing rate (FR) was measured using a slope/height window discriminator (FHC Model 700B). The reversibility of all electrophysiological responses under investigation was verified by a return to baseline values upon change of the solution back to normal aCSF. When two sequential hypercapnic exposures were studied, current was injected via an Axopatch 200B amplifier to ensure that all normocapnic (resting) firing rates remained within 0.5 Hz of initial recorded values in order to accurately compare both chemosensitive responses. V_m was corrected for the liquid junction potential (16 mV calculated from the Henderson equation using Clampex). Capacitance values (C_m) for LC neurons were measured in current-clamp mode according to the method of Golowasch et al. (2009). In brief, DC current pulses (I_{ext}, −50 to −200 pA, 800 ms) were applied from a membrane potential without firing activity (around −70 mV), and the resulting hyperpolarization (10–20 mV) was recorded. Four consecutive traces in each neuron were averaged to remove noise. In order to get the membrane time constant (τ_m) and the change of

Table 1. Values of arterial pH (pHa), arterial carbon dioxide partial pressure (Pa_{CO2}), arterial oxygen partial pressure (Pa_{O2}) and plasma bicarbonate (HCO_3^-) of Wistar rats in vehicle (aCSF) and Paxilline (100 μM or 500 μM) groups before microinjection (b.m.) and 30 min after microinjection (a.m.) during normocapnia (A); and before microinjection (Normocapnia) and 30 min after microinjection during hypercapnia (B)

A.	aCSF (n = 5)		Paxilline 100 μM (n = 6)		Paxilline 500 μM (n = 6)	
	Normocapnia (b.m.)	Normocapnia (a.m.)	Normocapnia (b.m.)	Normocapnia (a.m.)	Normocapnia (b.m.)	Normocapnia (a.m.)
pHa	7.43 ± 0.01	7.43 ± 0.01	7.43 ± 0.01	7.43 ± 0.01	7.44 ± 0.01	7.43 ± 0.01
$PaCO_2$ (mmHg)	29.7 ± 1.2	29.9 ± 1.6	27.6 ± 1.9	29.2 ± 1.3	29.9 ± 1.7	28.7 ± 1.6
PaO_2 (mmHg)	78.4 ± 1.5	80.6 ± 0.6	81.5 ± 1.3	80.1 ± 1.9	80.8 ± 2.0	81.6 ± 2.1
HCO_3^-	20.0 ± 1.0	20.8 ± 1.0	18.7 ± 1.3	19.6 ± 1.0	20.7 ± 1.6	19.5 ± 1.5

B.	aCSF (n = 7)		Paxilline 100 μM (n = 8)		Paxilline 500 μM (n = 9)		Paxilline peri-LC (n = 6)	
	Normocapnia	Hypercapnia	Normocapnia	Hypercapnia	Normocapnia	Hypercapnia	Normocapnia	Hypercapnia
pHa	7.44 ± 0.01	7.30 ± 0.01*	7.43 ± 0.01	7.31 ± 0.01*	7.42 ± 0.01	7.28 ± 0.01*	7.44 ± 0.01	7.31 ± 0.01*
$PaCO_2$ (mmHg)	30.2 ± 1.1	45.4 ± 1.7*	27.7 ± 1.8	43.5 ± 1.6*	28.1 ± 1.4	44.4 ± 1.4*	30.3 ± 0.6	45.7 ± 2.8*
PaO_2 (mmHg)	81.7 ± 1.9	117.0 ± 2.0*	78.5 ± 1.8	112.0 ± 1.9*	82.9 ± 1.4	110.1 ± 1.7*	80.2 ± 2.0	109.2 ± 3.6*
HCO_3^-	20.5 ± 0.9	22.5 ± 0.7*	18.6 ± 0.9	21.9 ± 0.9*	18.6 ± 1.0	21.0 ± 0.8*	20.9 ± 0.6	23.3 ± 1.8*

* Means statistically different between the time before microinjection and 30 min after microinjection in the same group (P < 0.05, *One-way* ANOVA).

membrane potential (V_m, not the input resistance of the neuron), the averaged trace was fitted from t = 0 to a time at which the voltage had reached steady state with two or three exponential terms using the Lenenberg-Marquardt (LM) algorithm of the Clampfit analysis software in the pClamp package. C_m is obtained by dividing τ_m by the resistance coefficient R_m ($= V_m/I_{ext}$):

$$C_m = \tau_m/R_m = \tau_m I_{ext}/V_m.$$

For voltage-clamp experiments, LC neurons were clamped at −70 mV in aCSF and equilibrated with 5% CO_2/95% O_2 or 15% CO_2/85% O_2 as indicated. 1 μM TTX was added to block Na^+ currents. For Ca^{2+} currents, 3 mM $BaCl_2$ was added in the perfusate as the charge carrier through voltage dependent calcium channels, and 3 mM 4-AP was added to block transient potassium channels. Step-wise depolarizations of 600-ms duration in 10 mV increments from −70 mV to +50 mV were applied and the resulting peak current measured. For BK currents, neurons were clamped at −70 mV, followed by a step depolarization to +10 mV for 40 ms to achieve Ca^{2+} loading in the neuron (pre-pulse), and immediately followed by a step depolarization to +80 mV to record the BK currents as well as any voltage-activated K^+ and Ca^{2+} currents. This double-pulse protocol was repeated following a 3-min exposure to 1 μM paxilline, and the resulting currents subtracted to obtain the BK difference current (Pax ΔI). For BAPTA experiments, the brain slice containing the LC was incubated in room-temperature aCSF containing 40 μM BAPTA-AM for 25 min prior to use. The series resistance was always 60–70% compensated. The membrane potential was corrected for the liquid junction potential. The membrane steady-state leak current was subtracted with Clampfit software.

Surgeries and microinjection

Ventilatory experiments were performed on unanesthetized male Wistar adult rats weighing 300–350 g. Rats had free access to water and food and were housed in a temperature-controlled chamber maintained at 24–26 °C (ALE 9902001; Alesco Ltda., Monte Mor, SP, Brazil) with a 12:12 light:dark cycle (lights on at 7:00 am). All surgical procedures were performed under anesthesia with 100 mg/kg of ketamine (Union National Pharmaceutical Chemistry S/A, Embu-Guaçu, SP, Brazil) and 10 mg/kg of xylazine (Laboratories Calier S/A, Barcelona, Spain), administered intraperitoneally. All procedures were similar to those previously used to bilaterally microinject drugs into the LC (Patrone et al., 2014).

The head was shaved, and the skin was sterilized with betadine solution and alcohol. Rats were fixed to a Kopf stereotaxic frame and implanted with a stainless steel guide cannula. Two guide cannulae (each 0.7 mm o.d. and 15 mm in length) were bilaterally implanted 1 mm above the LC region (distance from lambda: anterior: −3.4 mm; lateral: either −1.2 mm or +1.2 mm; and dorsal: −5.8 mm deep from the skull and inclination of vertical stereotaxic bar at 15°), according to the Paxinos and Watson atlas (Paxinos and Watson, 2005). The two cannulae were attached to the bone with stainless steel screws and acrylic cement. A tight-fitting stylet was kept inside each of the guide cannulae to prevent occlusion. After surgery, animals were treated with antibiotic (enrofloxacin, 10 mg/kg, intramuscular) and analgesic (flunixin meglumine, 2.5 mg/kg, subcutaneous) agents. Experiments were performed 7 days after surgery.

One day before the experiments, rats underwent two surgeries under tribromoethanol anesthesia. First, a catheter [PE-10 connected to PE-50 (Clay Adams, Parsippany, NJ, USA)] was inserted into the abdominal aorta through the femoral artery to measure pulsatile arterial pressure (PAP). The catheter was tunneled subcutaneously and exteriorized through the back of the neck. On the following day, this catheter was connected to the pressure transducer in a way that allowed free movement of the rat. For body temperature (Tb) measurements, a temperature datalogger (SubCue Data

Loggers) was implanted in the abdominal cavity through a midline laparotomy. The datalogger was programmed to acquire data every 5 min. These temperature values were used to calculate pulmonary ventilation.

A 5-μL Hamilton syringe and a dental injection needle (Mizzy, 200 μm o.d.) connected to a PE-10 tube were used to perform the microinjections into the LC of unanesthetized rats. The injection needle was 1 mm longer than the guide cannula so that the LC was reached by the needle only at the time of injection. The injection needle was placed into one of the guide cannulae and a volume of 100 nL of vehicle or drug solution was injected over a period of 30 s. Following the injection, the needle was removed from the guide cannula after an additional 20 s to avoid reflux. The injection needle was then placed into the other guide cannula and the injection process was repeated. Thus, both injections took a total time of about 2 min. All injections were performed using a microinjector machine (model 310, Stoelting CO) and during this process, the animal was free to move when the microinjection needle was inserted into the guide cannula, avoiding more stress.

Determination of physiological parameters

The ventilation ($\dot{V}_E$) measurements were taken by the barometric method (whole body plethysmography) as previously described (Bartlett and Tenney, 1970; Biancardi et al., 2008; Patrone et al., 2014; De Carvalho et al., 2010). The PAP was measured using a pressure transducer (TSD 104A, Biopac Systems, Goleta, CA, USA) connected to an amplifier (DA 100C, Biopac Systems, Goleta, CA, USA). Heart rate (HR) and mean arterial pressure (MAP) were quantified from the PAP records using the same system (MP100 ACE, Biopac Systems, Goleta, CA, USA). For pH and blood gases measurements, two drops of blood were sampled for immediate analysis of arterial pH (pHa), arterial carbon dioxide partial pressure (Pa_{CO2}), arterial oxygen partial pressure (Pa_{O2}) and plasma bicarbonate (HCO_3^-). These samples were transferred to an EG7+ cartridge for use with an i-STAT blood gas portable analyzer (i-STAT Analyzer, Abbott Laboratories, Illinois, USA).

Experimental protocol

Rats were individually placed in a plexiglas chamber (5 L) with room temperature maintained at 25 °C and allowed to move freely while the chamber was flushed with humidified air during approximately 30 min. Rats were then exposed to a hypercapnic gas mixture (7% inspired CO_2 in air) or normocapnic air during 30 min, followed by a recovery time of 20 min under normocapnia.

After ~30-min acclimatization period, control $\dot{V}_E$, MAP, HR, Tb and blood gases were measured before the microinjection. Subsequently, 100 nL of vehicle (aCSF + 1% ethanol) or paxilline (100 μM or 500 μM) was microinjected bilaterally into the rat LC. The bilateral microinjections were made sequentially. Cardiorespiratory measurements were performed 2, 5, 10, 15, 20, 30 and 50 min after microinjection under normocapnic conditions. Thirty minutes after microinjection the second measurement of blood gases was performed. Core body temperature was measured at 5-min intervals throughout the experiment.

For the measurements of the effects of bilateral intra-LC paxilline microinjections on $\dot{V}_E$, MAP, HR and Tb in response to hypercapnia, experiments were performed similarly to those of the preceding protocol except for the timing of the microinjection. After the control $\dot{V}_E$, MAP, HR, Tb and blood gases measures, but before performing the microinjection, a hypercapnic gas mixture (7% inspired CO_2 in air) was flushed through the chamber for 10 min, pre-establishing a systemic hypercapnic condition at the time of the pharmacological blockade, and then rats received bilateral microinjections of 100 nL of vehicle (aCSF + 1% ethanol) or paxilline (100 μM or 500 μM) into the LC. Exposure to hypercapnia was followed by a recovery time of 20 min under normocapnia.

During the whole animal plethysmography experiments, the mean temperature inside of the chamber was 26.9 ± 0.3 °C and the mean room temperature was 24.7 ± 0.1 °C.

Histology

Following completion of the experiments, the animals were deeply anesthetized with intraperitoneal injection of ketamine and xylazine and a needle injector (33 gauge) was inserted through the guide cannula and a 100 nL microinjection of Evan's blue was performed. Subsequently, animals were transcardially perfused with saline followed by 10% formalin solution. Brains were removed and post-fixed in 10% buffered formalin solution for at least 2 days.

After fixation, the brainstems were embedded in paraffin, sectioned on a microtome (15-μm-thick coronal sections) and stained by the Nissl method to visualize the region of the microinjection under light microscopy. The region of microinjection was determined using the atlas of Paxinos and Watson (2005) as a reference. Only rats with a confirmed site of bilateral microinjection in the LC were considered for the intra-LC group while rats with microinjection sites located surrounding the LC were considered for the peri-LC group.

Drugs

For in vitro experiments, TTX, BAPTA-AM, paxilline, nifedipine, BSA, and Fura-2 were purchased from Sigma–Aldrich (St Louis, MO, USA). Nifedipine and paxilline were prepared as stock solutions in ethanol (50 mM and 10 mM, respectively). BAPTA-AM stocks (10 mM) were prepared in DMSO, and TTX and Fura-2 stocks (1 mM and 10 mM, respectively) were in dH_2O. For *in vivo* experiments, paxilline was prepared as a stock solution (10 mM) in ethanol and before an experiment was diluted in aCSF to a final concentration of either 100 μM or 500 μM.

Data analysis and statistics

The firing rate of LC neurons was calculated as the integrated firing rate over a 10-s bin. Thus, the number

of action potentials was determined for each 10 s of the V_m trace and plotted as the number of action potentials per second (Hz) in the ∫Firing Rate vs. time plots. At least 10 integrated firing rate values were averaged to get a firing rate (FR) value for a given condition. Where applicable, analysis for the change in firing rate (ΔFR) was calculated by the following: ΔFR = (hypercapnic average firing rate − control average firing rate). This gives the absolute increase in firing rate in response to various hypercapnic challenges as an increase in firing rate during hypercapnia minus the control firing rate.

All values are expressed as mean ± SEM. Significant differences between two means were determined by Student's *t*-tests or paired *t*-tests. Comparisons of more than two means were assessed using ANOVA with multiple paired comparisons. For ventilatory, cardiovascular and blood gas analyses, the normocapnic and hypercapnic conditions were analyzed separately to determine the effect of drug microinjection. The effect of hypercapnia on V_T, f_R, $\dot{V}_E$, MAP, HR and Tb over the time course was evaluated by a two-way analysis of variance (repeated measures). For blood gases and pH, since an interaction (time × treatment) was observed, point-by-point comparisons of mean values between vehicle and drug treatments during normocapnia and hypercapnia were performed by a one-way ANOVA. All statistical analyses were performed using SigmaPlot 11 (Systat Software, Inc.). Differences were considered significant if $P < 0.05$.

RESULTS

Development of L-type Ca^{2+} currents in LC neurons from neonates

In the present study, whole-cell voltage clamp of LC neurons in the presence of Na^+ and K^+ channel blockade demonstrated prolonged inward currents (mediated by barium influx) that were evoked by step pulses from a holding potential of −70 mV to +50 mV in 10 mV increments (Fig. 1A). This current was larger in LC neurons from rats aged P13 (about 2 nA) than in neurons from rats aged P5 (about 1 nA) (Fig. 1A). The plot of current density (pA/pF) vs. voltage showed an inverted bell-shaped curve with activation at −40 mV and a peak at 0 to +10 mV, consistent with a Ca^{2+} current (Fig. 1B). These curves are similar to those previously measured in enzyme-dissociated single LC neurons from neonatal rat pups (P3–P9) (Chieng and Bekkers, 1999).

The long inactivation time (>200 ms) and high activation threshold (around −40 mV) of this current is consistent with the activity of L-type Ca^{2+} channels. In the present study, this inactivation was minimal due to the addition of 10 mM EGTA to the intracellular pipette solution, and the majority of the Ca^{2+} current inactivated slowly if at all (Fig. 1A).

During the first two weeks after birth, the membrane capacitance of LC neurons increased by about 40% from 114.02 ± 7.78 pF ($n = 5$) in neurons from rats aged P3–P4, to 147.53 ± 8.99 pF ($n = 5$) in neurons from rats aged P9, to 157.68 ± 8.98 pF ($n = 8$) in rats aged P13–P14. This suggests that these neurons increase in size during the first 2 weeks of life (Warren and Jones, 1997; Suwabe et al., 2011). During the same time period, there was a significant ($P < 0.05$) increase in the peak Ca^{2+} current density of about 25% from 10.21 ± 0.63 pA/pF ($n = 5$) in neurons from rats aged P3–P4 to 12.59 ± 0.51 pA/pF ($n = 5$) in neurons from rats aged P13 to P14 (Fig. 1B. inset). These data are consistent with our prior findings of an increase in an L-type Ca^{2+} current in LC neurons over this age period (Imber and Putnam, 2012).

To evaluate the possible contribution of L-type channels to the Ca^{2+} current in LC neurons, nifedipine (50 μM), an L-type Ca^{2+} channel inhibitor, was applied (Fig. 1C). In four neurons older than P8, the total Ca^{2+} current was significantly ($P < 0.01$) reduced by over 60% after 9 min of exposure to nifedipine, from 2284 ± 572 pA in the absence of nifedipine to 868 ± 228 pA in its presence. These findings support a significant contribution from L-type Ca^{2+} channels to the measured current (Fig. 1C, inset). Thus, our results suggest that the bulk of Ca^{2+} current in postnatal LC neurons is due to L-type Ca^{2+} channels.

Effect of hypercapnic acidosis on Ca^{2+} currents and intracellular Ca^{2+}

We directly tested the possibility of Ca^{2+} channels being activated by hypercapnic acidosis in LC neurons by testing the effect of 15% CO_2 on Ca^{2+} currents in LC neurons. Hypercapnic acidosis increased the inward current in response to a depolarizing pulse from a holding potential of −70 mV to −10 mV (Fig. 1D). In seven LC neurons aged between P7 and P10, hypercapnic acidosis caused marked changes in the peak amplitude of the Ca^{2+} current (Fig. 1E), increasing significantly ($P < 0.01$) in response to an increase in CO_2 from 5% to 15% (Fig. 1F). Thus, hypercapnic acidosis can activate the Ca^{2+} current in LC neurons from neonatal rats.

Since hypercapnic acidosis activates Ca^{2+} channels in LC neurons, we determined whether it can also lead to increased Ca_i^{2+} levels. We measured the intracellular Ca^{2+} levels using the Ca^{2+}-sensitive fluorescent dye Fura-2. Current clamp of LC neurons under these conditions revealed normal resting V_m of −40 to −45 mV and firing rates of 1–4 Hz in 5% CO_2, in agreement with previous studies (Filosa and Putnam, 2003; Ritucci et al., 2005b). Simultaneous fluorescence imaging of the patched neuron showed stable resting Ca_i^{2+} levels as indicated by stable R_{fl} values for Fura-2 (Fig. 2A). When the neuron was exposed to hypercapnic acidosis, firing rate increased as expected. Concurrent with the increase in firing rate, the observed R_{fl} values also increased, indicating a rise in the average Ca_i^{2+} during hypercapnia (Fig. 2A). When 5% CO_2 was restored, Ca_i^{2+} (R_{fl}) returned to resting levels. Fig. 2B summarizes the results for the average increases in R_{fl} (Ca_i^{2+}) in LC neurons from rats younger ($n = 13$) and older ($n = 6$) than P10. Note that resting levels of Ca_i^{2+} (in 5% CO_2) are significantly larger in the older neonates (Fig. 2B), which is in agreement with a larger resting Ca^{2+} current in older neonates (see Fig. 1B, inset).

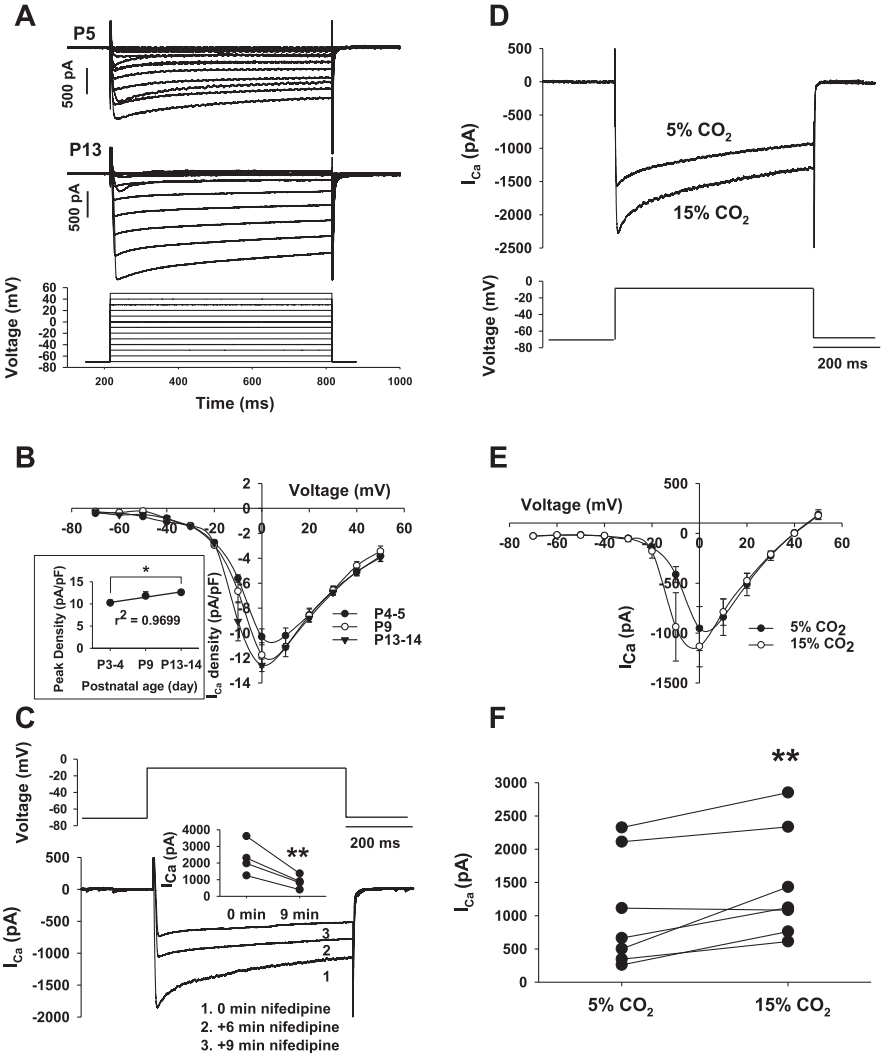

Fig. 1. The Ca^{2+} current in LC neurons from neonatal rats: the effects of neonatal age, nifedipine and hypercapnic acidosis. (A). Voltage-sensitive currents activated by +10 mV steps from −70 mV to +50 mV in the presence of Na^+ and K^+ blockade and 3 mM $BaCl_2$ (to carry Ca^2 current). (Top trace) A typical result for neurons from a P5 rat; (middle trace) characteristic of neurons from an older (P13) rat. Note the large difference in the amplitude of inward current; (bottom trace) the voltage-clamp protocol used to obtain the currents. (B). I–V plots of current densities vs. voltage for LC neurons from rats in three different age groups. The resulting I–V plots are characteristic for high voltage activated Ca^{2+} channels, such as L-type. The filled black circles represent points from rats aged P3 to P4 (n = 5), open circles are points from rats aged P9 (n = 5), and black triangles are points from rats aged P13 to P14 (n = 5). The current amplitude increases as neonatal rats age. *Inset:* The peak Ca^{2+} current densities increased with postnatal age and the peak densities were significantly different in LC neurons from rats aged P13 to P14 than in rats aged P3–P4. The peak Ca^{2+} current densities for LC neurons from intermediate aged rats (P9) were between the values for P3–P4 and P13–P14 rats but were not significantly different from either. $^{*}P < 0.05$. (C). The effect of the L-type Ca^{2+} channel inhibitor nifedipine on voltage-clamp recordings of the peak Ca^{2+} current from neonatal rats. Recordings were taken prior to the addition of nifedipine (0 min, 1), 6 min after addition (2), and 9 min after addition (3). *Inset:* The effect of nifedipine on peak Ca^{2+} current in LC neurons from rats aged P8 to P13 (n = 4). By 9 min, the peak current amplitude had been significantly reduced by over 60%. These results indicate that the majority of the Ca^{2+} current in LC neurons is due to the activity of L-type channels. $^{**}P < 0.01$. (D). The effect of hypercapnic acidosis on the Ca^{2+} current in an LC neuron from a P7 rat. Ca^{2+} currents were induced by a voltage step from a holding potential of −70 mV to −10 mV. Note the large increase in current amplitude at −10 mV in the presence of hypercapnic acidosis. (E). Comparison of two I–V plots recorded in LC neurons from rats aged P7 to P10 (n = 7) during exposure to 5% and 15% CO_2. The peak current amplitude increased by some 0.2 nA in hypercapnic acidotic solution. (F) Comparison of the average peak Ca^{2+} current amplitude recorded in both 5% and 15% CO_2 from 7 LC neurons from rats aged P7 to P10. Hypercapnic acidosis caused a highly significant increase in peak Ca^{2+} current in these neurons. $^{**}P < 0.01$.

Hypercapnic acidosis induces a significant increase in intracellular Ca^{2+} in both younger and older neonates as well (Fig. 2B). Since our data indicate that Ca^{2+} currents in LC neurons are predominantly L-type (see Fig. 1), the hypercapnic pulse was repeated in five neurons (from rats aged P7 to P13) in the presence of nifedipine. In each case, neurons were exposed to 50 μM nifedipine for at least 10 min, and within five minutes Ca_i^{2+} levels had begun to decrease (data not shown). In the presence of nifedipine, there was no increase in R_{fl} values during exposure to hypercapnic acidosis (Fig. 2B). Thus, our findings show that hypercapnic acidosis results in an increase in intracellular Ca^{2+} and suggest that this higher level of Ca_i^{2+} is due to activation of L-type Ca^{2+} channels.

Presence, activation and development of K_{Ca} channels in LC neurons

In the present study, we tested the presence of and the development of K_{Ca} channels in LC neurons with voltage clamp. A two-step voltage-clamp protocol, similar to a method used to study BK currents in chromaffin cells (Marcantoni et al., 2010), was used (Fig. 3). First, a "pre-pulse" step to +10 mV (from a holding potential of −70 mV) initiated Ca^{2+} loading into the neuron. Then a second, prolonged step to +80 mV activated voltage-sensitive currents (in the presence of Na^+ channel blockade) (Fig. 3A). The neuron was exposed to the BK channel inhibitor paxilline for 3 min, and the two-step protocol repeated. The difference current in the absence vs. the presence of paxilline was referred to as the paxilline-sensitive current, or the BK current (I_{BK}). This putative BK current was found to be non-inactivating (Fig. 3B), similar to the "slowly inactivating" BK current type noted in chromaffin cells (Marcantoni et al., 2010). An I–V plot of the I_{BK} showed an outwardly-rectified current that has a threshold for voltage activation at around −10 mV (Fig. 3C).

In order to study the development of the BK current in LC neurons, the maximum BK channel current

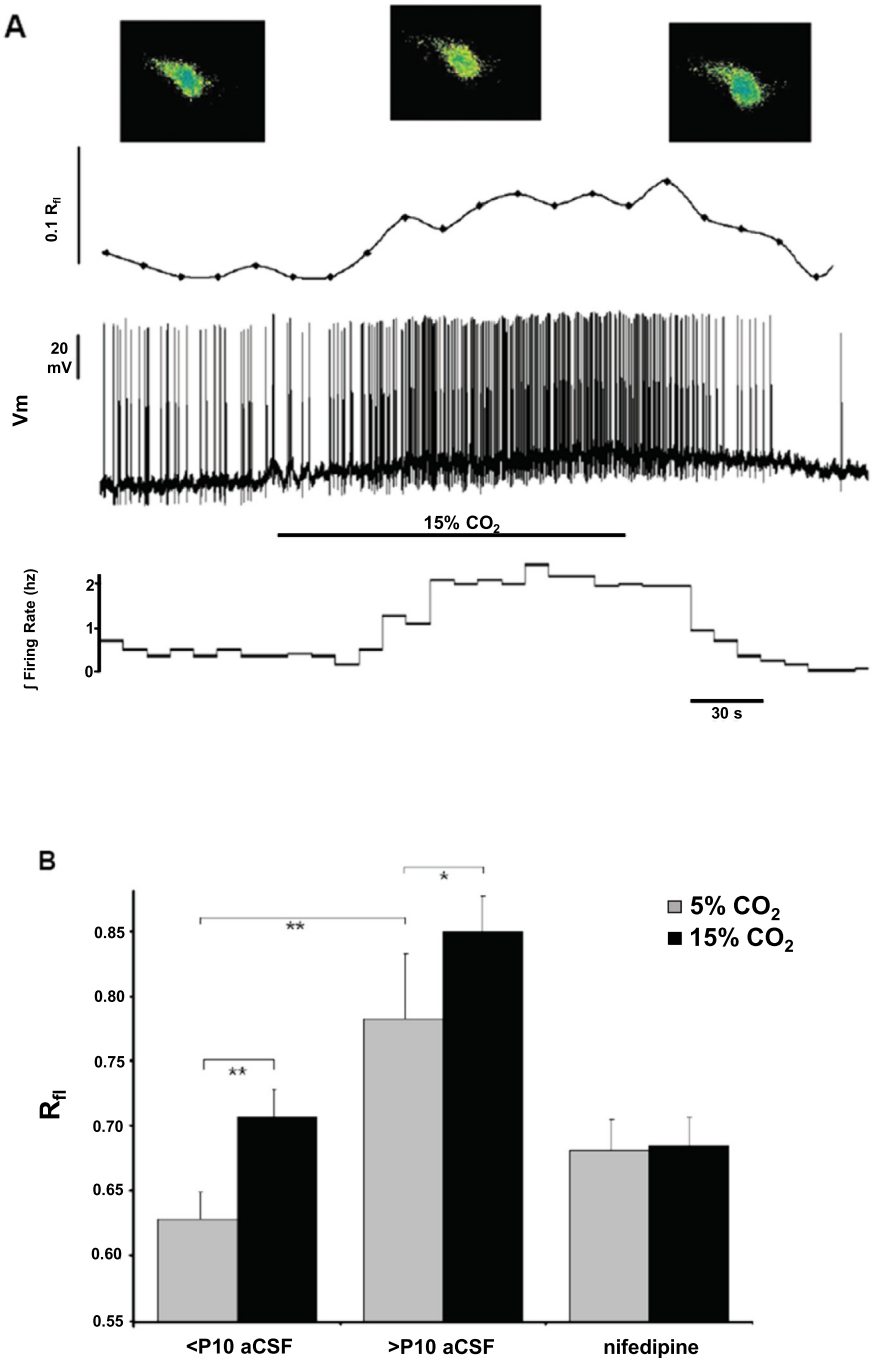

Fig. 2. The effect of hypercapnic acidosis on the firing rate and on intracellular Ca^{2+} concentration in LC neurons from neonatal rats. (A). Exposure to hypercapnic acidosis causes a reversible increase in firing rate and a concurrent increase in Ca_i^{2+}. (Upper panel) LC neuron loaded intracellularly with the Ca^{2+}-sensitive fluorescent dye Fura-2. Images are the ratio of fluorescence from excitation at 340 nm/380 nm (R_{fl}) in normocapnia (left panel), hypercapnia (middle panel) and upon return to normocapnia (right panel). The plot below these images are the values for R_{fl} at different time points (corresponding to the V_m trace below). Note that the R_{fl}, and therefore intracellular Ca^{2+}, increases reversibly during exposure to hypercapnia. (Lower panel) Whole-cell current-clamp patch of the depicted LC neuron showing a typical hypercapnic acidosis response of a reversible increase in firing rate upon exposure to 15% CO_2 shown as a reversible increase in the integrated firing rate (in Hz, action potentials/s) (bottom panel). Scale bars represent 200 μm. (B). Comparison of the relative changes in R_{fl} between normocapnic (5% CO_2) and hypercapnic acidotic (15% CO_2) aCSF. In LC neurons from both younger (<P10, $n = 13$) and older (>P10, $n = 6$) postnatal rats, there was a significant increase in Ca_i^{2+} during hypercapnia. Repeating these experiments in 5 LC neurons aged P7–P13 in the presence of nifedipine prevented the hypercapnic acidosis-induced increase in Ca_i^{2+}. Average normocapnic R_{fl} values were also found to increase between neurons from younger and older rats. $^{*}P < 0.05$; $^{**}P < 0.01$.

density was measured across neonatal age, and a significant increase in BK channel current density with age was found. LC neurons from rats aged P3 to 4 had BK channel current density of 4.80 ± 0.33 pA/pF ($n = 4$), from age P7 to 9 had BK current density of 8.40 ± 0.87 pA/pF ($n = 3$), and from age P13 to 15 had BK current density of 12.03 ± 0.87 pA/pF ($n = 3$; $P < 0.05$ compared to P3-4) (Fig. 3D). Thus, both Ca^{2+} and BK channel current density appears to increase in LC neurons during the first two neonatal weeks, consistent with an increased expression of both channels during development.

We have assumed that the BK channels are being activated by increased Ca_i^{2+} resulting from activation of L-type Ca^{2+} channels. We therefore tested the effect of nifedipine (50 μM) in LC neurons from older neonatal rats (P12). Nifedipine significantly inhibited I_{BK} by nearly 75% ($P < 0.001$) (Fig. 3E, F). Further, loading LC neurons with the Ca^{2+} chelator, BAPTA, also resulted in a significant inhibition of I_{BK} by about 75% ($P < 0.001$) (Fig. 3F), which is similar to the effect of nifedipine. Taken together, these results suggest a close functional relationship between L-type Ca^{2+} channels and BK channels in LC neurons.

The role of BK channels as a chemosensitive brake

To directly test the hypothesis that BK channels result in a braking phenomenon in LC neuron firing rate in response to hypercapnic acidosis, we studied the response of firing rate to 15% CO_2 in the absence and in the presence of 1 μM paxilline (a BK channel inhibitor) in LC neurons from neonatal rats (Fig. 4A). An LC neuron patched in current clamp was first exposed to hypercapnic acidosis in the absence of paxilline and the change in firing rate (ΔFR) determined. It was then exposed to paxilline for at least five minutes and the hypercapnic acidotic exposure repeated to determine the change in firing rate in the presence of BK channel inhibition (ΔFR_{pax}). Sample records of such experiments in LC neurons from rats of different age are shown in Fig. 4A. In an LC neuron

from a young rat (P6) (Fig. 4A, upper left panel), exposure to hypercapnic acidosis in the absence of paxilline resulted in an increase in firing rate by ~0.6 Hz and this magnitude of chemosensitivity was not much changed in the presence of paxilline. In an LC neuron from a P10 rat, a smaller chemosensitive response (ΔFR of ~0.3 Hz) was observed, and the addition of paxilline increased the ΔFR to about 0.9 Hz (Fig. 4A, upper right panel). This increase in the magnitude of the chemosensitive response by paxilline became more pronounced in LC neurons from older neonatal rats (P16) (Fig. 4A, middle panels). Here, the neuron showed a small hypercapnic acidotic response, with a ΔFR of ~0.1 Hz (Fig. 4A, middle left panel). When the neuron was exposed to paxilline, the hypercapnic acidotic response became much greater, with a ΔFR of ~2.8 Hz (Fig. 4A, middle right panel). Notably, the addition of paxilline to LC neurons from rats of all ages did not alter the basal firing rate in 5% CO_2 (Fig. 4A, lower left panel), suggesting that at most minor BK channel activity is present in resting LC neurons so that their inhibition by paxilline does not affect the firing rate. These data indicate that BK channels do serve a braking function on the hypercapnic acidosis-induced firing rate response of LC neurons from older neonates.

To compare the role of the chemosensitive braking function of BK channels in LC neurons across postnatal age, the hypercapnic acidosis-induced increase in firing rate in the absence of paxilline (ΔFR) was subtracted from the hypercapnic acidosis-induced increase in firing rate in the presence of paxilline (ΔFR_{pax}). The result was expressed as ($\Delta FR_{pax} - \Delta FR$) (Fig. 4B). In addition, another thirteen neurons were exposed twice to the same hypercapnic acidosis (15% CO_2) without the addition of paxilline, and the second hypercapnic acidosis-induced increase in firing rate (ΔFR_2) had the first firing rate (ΔFR_1) subtracted from it and the difference ($\Delta FR_2 - \Delta FR_1$) served as a control for the repeatability of the firing rate response to hypercapnia. This value was not significantly different when two control exposures to hypercapnic acidosis were given in the same neuron, indicating that our measurements of the firing rate response of LC neurons to hypercapnia are repeatable measures (Fig. 4B). Paxilline significantly increased the hypercapnia-induced elevated firing rate in LC neurons from young neonates (P5–P9), but the paxilline-induced increase was nearly 3× larger in neurons from older neonates (P10–P16) (Fig. 4B). These findings are consistent with BK channels operating as a brake that develops during the first two neonatal weeks and that limits the firing rate response of LC neurons to hypercapnic acidosis.

The development of the braking function should result in a decrease in the magnitude of the chemosensitive response of LC neurons to hypercapnic acidosis. In fact, the chemosensitivity of LC neurons (as measured by CI %) from postnatal animals ages P3–P5, P6–P9, and older than P10 shows a dramatic and significant decrease with increased age (Fig. 5A). The average CI values from younger neonates P3–P5 were about 210%, while neurons from animals older than P10 had significantly smaller CI values (around 125%). In addition, a transition period was evident from postnatal age P6–P9 where the CI values were usually around 160% (Fig. 5A). To study the relationship between the fall of CI% and the increase of BK channel current density in LC neurons during the neonatal period, we showed that the two parameters are highly correlated ($R^2 = 0.9838$), with CI% falling in inverse relationship to the increase in BK channel current density (Fig. 5B). The strong correlation suggests a relationship between the development of the BK current in LC neurons and the decrease in the average firing rate response to hypercapnic acidosis.

The effect of 10% and 7.5% CO_2 in activating the chemosensitive brake in LC neurons from neonatal rats

While 15% CO_2 is useful for maximizing the effects of hypercapnia, we were concerned that it represents a very high level of CO_2. We thus did studies using 10% and 7.5% CO_2 as more modest hypercapnic acidotic challenges to see if the braking phenomenon was still activated under these conditions.

We characterized the magnitude of the braking phenomenon by plotting the hypercapnic acidosis-induced ΔFR in the absence versus the presence of paxilline at different levels of hypercapnic acidosis (Fig. 6). The brake (the difference between the firing rate in the presence vs. the absence of paxilline) was much larger at higher levels of hypercapnic acidosis (addition of 5% or 10% CO_2, that correspond to final levels of 10% or 15% CO_2, respectively) than when hypercapnic acidosis is much smaller (addition of 2.5% CO_2, that correspond to final level of 7.5% CO_2) (Fig. 6). These findings indicate that the brake may only play a major role in ventilatory control under conditions involving large hypercapnic values, but may not play a role in the control of breathing in response to lower levels of hypercapnia.

Effect of bilateral LC injection of paxilline on cardiorespiratory responses of adult rats to hypercapnia

We directly tested whether the braking pathway does play a role in the breathing response to hypercapnia. Fig. 7 is a representative photomicrograph of a transverse section of rat brainstem that includes the LC region (dashed red circles), showing an example of a typical bilateral intra-LC injection. The microinjection regions (circled in red) show the specificity of the microinjection to the LC. Fig. 8 shows line drawings of several injection sites including both intra-LC and peri-LC injections. On the left are the injections into the LC region (Fig. 8A), while on the right are drawings showing the injections surrounding the nucleus that missed the LC altogether (Fig. 8B).

Table 1 shows the effects of paxilline intra-LC and peri-LC (100 μM and 500 μM) or vehicle microinjections on pHa, Pa_{CO2}, Pa_{O2}, and plasma HCO_3^- under normocapnic (Table 1A) and hypercapnic (Table 1B) conditions. Under

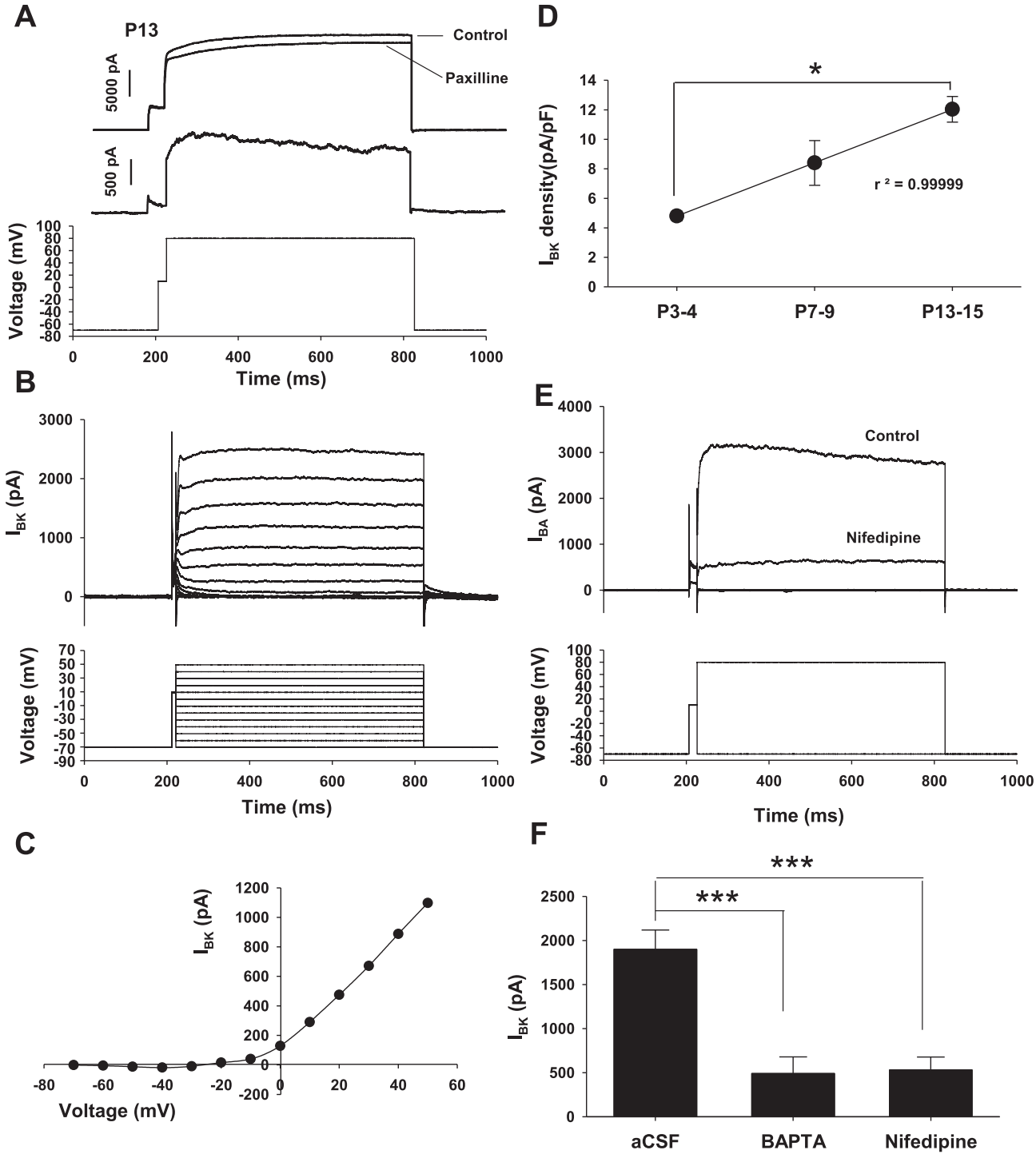

Fig. 3. Measurement of BK channel activity as a paxilline-sensitive and Ca-dependent current in LC neurons from neonatal rats of different ages Whole-cell voltage-clamp recordings in the presence of TTX. (A). (Upper trace) Records from a > P10 rat showing activation of voltage-sensitive currents with and without the presence of the BK channel inhibitor, paxilline (1 μM). (Middle trace) The subtraction of the two upper traces, representing the paxilline-sensitive current, or Pax ΔI. Under the conditions of activation, the Pax ΔI did not exhibit inactivation. (Lower trace) The voltage step to + 80 mV was preceded by a brief step to + 10 mV to initiate an increase in Ca_i^{2+} (pre-pulse). (B). Pax Δ*I* (I_{BK}) evoked by 10 mV step-wise voltages from −70 mV to + 50 mV, all preceded by a pre-pulse step to + 10 mV. (C). A figure of the resulting I–V plot of the peak Pax Δ*I* (I_{BK}) currents as derived from records as shown in B. (D). Plot of average peak Pax ΔI current densities over three age groups: P3–P4 (n = 4), P7–P9 (n = 3), and P13–P15 (n = 3), as measured in voltage clamp with a pre-pulse to + 10 mV and a voltage step to + 80 mV. The Pax ΔI (BK current) density increased significantly from the youngest age group to the oldest. $^{*}P < 0.05$. (E). (Upper trace) Pax Δ*I* (I_{BK}) recorded from a LC neuron from a P12 rat with and without the presence of nifedipine (50 μM). (Lower trace) A representation of the voltage steps. Nifedipine caused a significant decrease in amplitude of the Pax Δ*I*. (F). Comparison of the average peak Pax Δ*I* (I_{BK}) (n = 17) following either incubation with 40 μM BAPTA-AM (n = 10) or in the presence of nifedipine (n = 11). Both BAPTA and inhibition of the L-type Ca^{2+} channel decreased the Pax Δ*I* (I_{BK}) amplitude by the same approximate amount. All data were from neonatal rats aged P10 to P14. $^{***}P < 0.001$.

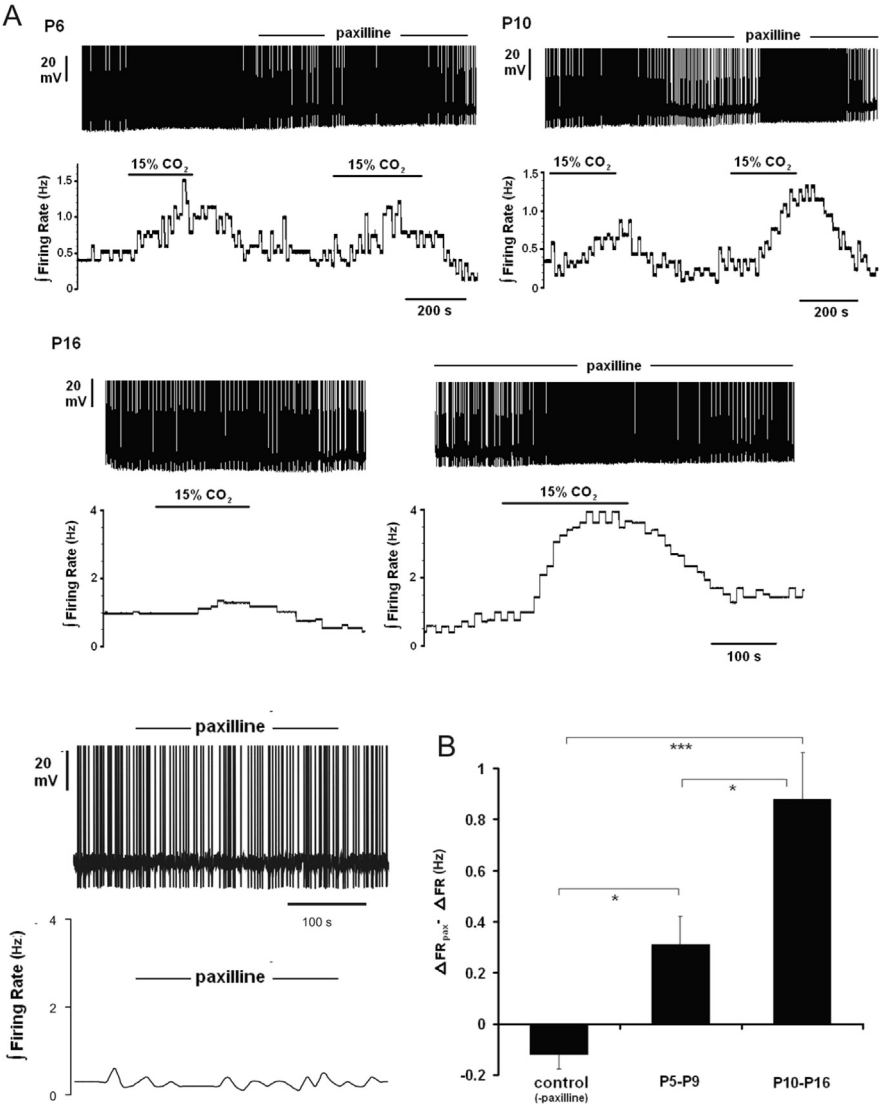

Fig. 4. The effect of paxilline on the firing rate response to hypercapnic acidosis of LC neurons in neonatal rats of different ages. (A). The inhibition of BK channels by paxilline causes an increase in the chemosensitive firing rate response of LC neurons to hypercapnic acidosis that is dependent on postnatal age. (Upper panels) Typical results for whole-cell current-clamp experiments from younger (P6) and older (P10) neonatal rats, comparing the firing rate response to hypercapnic acidosis with and without paxilline. Notice the lack of firing rate response to the addition of paxilline during normocapnia. Paxilline has very little effect on the firing rate response to hypercapnic acidosis in an LC neuron from a rat aged P6 (left panel) but increases the firing rate response somewhat in an LC neuron from a rat aged P10. (Lower panels) The same experiment on an LC neuron from a P16 neonatal rat is shown. Here, the chemosensitive response is characteristically low (left panel), and was increased significantly in the presence of paxilline (right panel). (Bottom left panel) An LC neuron in normocapnia (5% CO_2) has an unchanged integrated firing rate upon transient exposure to paxilline, suggesting that BK channels are not active in LC neurons in normocapnia. This tracing is representative of 3 such tracings where the firing rate, under normocapnic conditions, was the same in the absence (0.62 ± 0.32 Hz) and the presence (0.62 ± 0.53 Hz) of paxilline (the change in firing rate for the 3 neurons was 0.017 ± 0.032 Hz). (B). Summary of the results from comparisons of sequential responses to hypercapnic acidosis in LC neurons with (ΔFR_{pax}) and without (ΔFR) the presence of paxilline. ΔFR represents the difference in average firing rate (Hz) in the presence of 15% CO_2 and 5% CO_2. $\Delta FR_{pax} - \Delta FR$, then, measures the increase in the firing rate response to hypercapnic acidosis caused by inhibition of the braking pathway (see text). Control values represent sequential responses to hypercapnic acidosis without the addition of paxilline ($\Delta FR_2 - \Delta FR_1$). All values were significant from one another, and the results indicate a development of the braking pathway (control, $n = 13$; P5–P9, $n = 20$; P10–P16, $n = 14$). $^{*}P < 0.05$; $^{***}P < 0.001$.

normocapnic conditions, no changes in blood gas values, pHa or HCO_3^- were observed after vehicle or paxilline injection (Table 1A). Inspiration of air containing 7% CO_2, however, significantly increased Pa_{CO2} and Pa_{O2} ($P < 0.05$) and also decreased pHa ($P < 0.001$) in all groups (Table 1B). The values of plasma HCO_3^- were significantly increased above normocapnic levels during exposure to hypercapnia ($P < 0.05$), but not different between vehicle and treated groups (Table 1B). Under hypercapnic conditions, there were no differences in any of these variables among the injection groups (Table 1B).

The measurement of ventilatory parameters, cardiovascular parameters and T_b under normocapnic conditions showed that microinjection of vehicle or paxilline intra-LC (100 μM or 500 μM) had no effect on $\dot{V}_E$ (Fig. 9A), MAP, HR or T_b (Fig. 10A1–A3, respectively). Under hypercapnic conditions, as expected, we observed a significant increase in $\dot{V}_E$ in all groups, which resulted from increases of both f_R and V_T ($P < 0.001$) (Fig. 9B). However, the animals treated with paxilline (both concentrations of 100 μM and 500 μM) intra-LC resulted in a significant increase of the respiratory response to hypercapnia ($P < 0.001$) compared to rats injected with vehicle or paxilline peri-LC. This significantly increased ventilatory response to hypercapnia observed in the paxilline intra-LC groups was mainly due to an increase in V_T ($P < 0.001$), although significant increases also were observed in the f_R (mainly between vehicle and paxilline 100 μM intra-LC group) ($P < 0.01$) (Fig. 9B). Hypercapnia did not change MAP or HR (Fig. 10B1, B2; respectively). However, MAP was affected transiently by paxilline intra-LC microinjection (100 μM and 500 μM) increasing significantly during high levels of CO_2 ($P < 0.01$). HR was also transiently affected by both concentrations of paxilline, being significantly higher at 2 and 5 min after bilateral intra-LC microinjection ($P < 0.05$) compared to vehicle and paxilline peri-LC group (Fig. 10B1, B2).

Exposure to hypercapnia and microinjection of paxilline intra-LC and peri-LC (100 μM and 500 μM) did not cause changes in the body temperature (Fig. 10B3). However, the CO_2 sensitivity (Fig. 11) was significantly increased ($P < 0.05$) after 100 and 500 μM paxilline injection (103.2 ± 16.4 and 89.4 ± 8.4, respectively), compared to vehicle group (53.8 ± 3.9 mL^{-1} kg^{-1} min^{-1} $mmHg^{-1}$). In summary, bilateral injections of paxilline into the LC of rats resulted in no change in ventilation under normocapnic conditions but significantly increased the ventilatory response to hypercapnia. Bilateral injections of paxilline into the LC also enhanced the responses of MAP and HR to hypercapnia, but only transiently.

DISCUSSION

The major findings of this study are that: (1) hypercapnic acidosis activates L-type Ca^{2+} channels in LC neurons; (2) the activation of these channels increases intracellular Ca^{2+} which activates BK channels; (3) this pathway acts as a brake on the firing rate response of chemosensitive LC neurons to hypercapnic acidosis; (4) the development of this braking pathway accounts for the decrease in the magnitude of the firing rate response of LC neurons to hypercapnic acidosis during early development in rats; and (5) inhibition of BK channels in LC neurons results in a significant increase in the hypercapnic ventilatory response in rats, suggesting that this braking pathway helps to determine respiratory drive in response to hypercapnia. The braking pathway may represent a new mechanism for controlling the gain of the chemosensitive response of neurons to hypercapnic acidosis and alterations of this braking pathway may contribute to pathological conditions such as sleep apnea and panic disorder.

Activation of Ca^{2+} currents by hypercapnic acidosis

The inward current that we observed in LC neurons in the absence of fast Na^+ currents had a characteristic Ca^{2+} channel I–V plot (Fig. 1B, E). The current showed fast activation, very slow inactivation and substantial inhibition (over 60%) by nifedipine (Fig. 1A, C) suggesting that the bulk of the current was due to L-type Ca^{2+} channels. The current remaining in the presence of nifedipine also had very slow inactivation, suggesting it was also an L-type Ca^{2+} current. We do not know if this represents incomplete inhibition of the current by nifedipine, possibly due to slow penetration of the inhibitor into the slice, or if it represents heterogeneity among L-type Ca^{2+} channels (Lipscombe et al., 2004). Another possibility is that the residual Ca^{2+} current may be caused by TRP channels (Kunert-Keil et al., 2006; Cui et al., 2011). However, based on the increasing inhibition of Ca^{2+} current by nifedipine with exposure time (Fig. 1C), penetration of the inhibitor into the slice is clearly an issue. It is clear that LC neurons express L-type Ca^{2+} channels but the molecular identity of these channels must await future studies, most likely involving the use of single cell RT PCR.

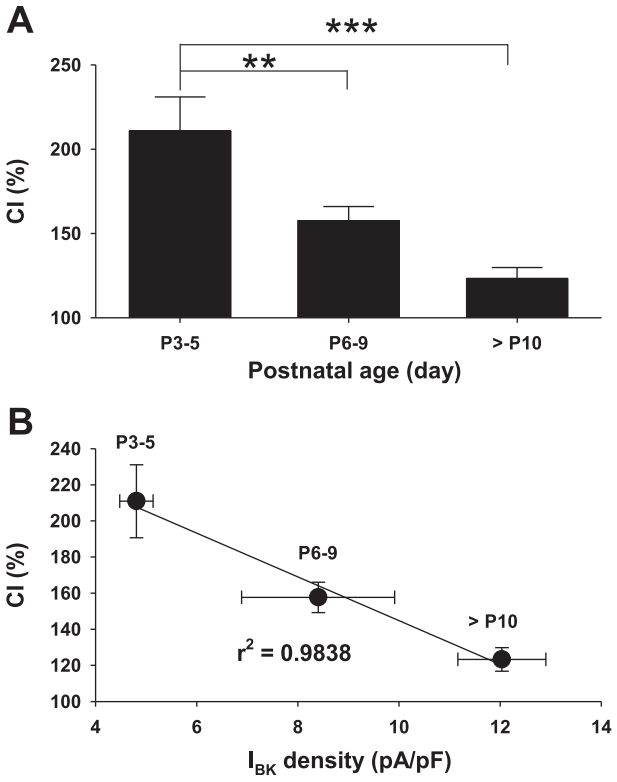

Fig. 5. The effect of neonatal rat age on the CI of LC neurons and its relationship with the BK current density. (A). Comparison of the chemosensitivity index (CI) of LC neurons across postnatal age P3–P5 ($n = 12$), P6–P9 ($n = 18$), and >P10 ($n = 36$) measured by whole-cell current-clamp studies. Results show a steady decrease in the firing rate response to hypercapnic acidosis of individual neurons over the first ~2 postnatal weeks. These findings support the development of a chemosensitive "brake" over this period (see text). $^{**}P < 0.01$; $^{***}P < 0.001$. (B). When the CI is plotted versus the average BK current density in LC neurons from rats of ages P3 to P16, an inverse relationship is observed. These results suggest that the development of the BK current in LC neurons may be responsible for the decrease in the firing rate response to hypercapnia in LC neurons from neonatal rats with increasing age. [$CI = -12.111(I_{BK}) + 265.83$, $R^2 = 0.9838$].

Exposure of LC neurons to hypercapnic acidosis resulted in an increase in the Ca^{2+} current (Fig. 1D–F). This agrees with previous work from our laboratory that showed that hypercapnic acidosis activates nifedipine-sensitive, TTX-insensitive Ca^{2+} currents in LC neurons, clearly indicating a pH-sensitive activation of Ca^{2+} currents (Filosa and Putnam, 2003; Imber and Putnam, 2012). However, this is in contrast to the H^+-sensitive inhibition of Ca^{2+} currents observed in other cell types, particularly high-voltage activated (HVA) currents such as L-type Ca^{2+} currents (Tombaugh and Somjen, 1997; Shah et al., 2001).

Activation of Ca^{2+} currents in LC neurons results in increased Ca_i^{2+}

Ca^{2+} spikes in LC neurons are capable of elevating intracellular Ca^{2+} in the soma (Imber and Putnam, 2012). We found a measurable increase in intracellular Ca^{2+} in LC soma induced by hypercapnia (Fig. 2A). This

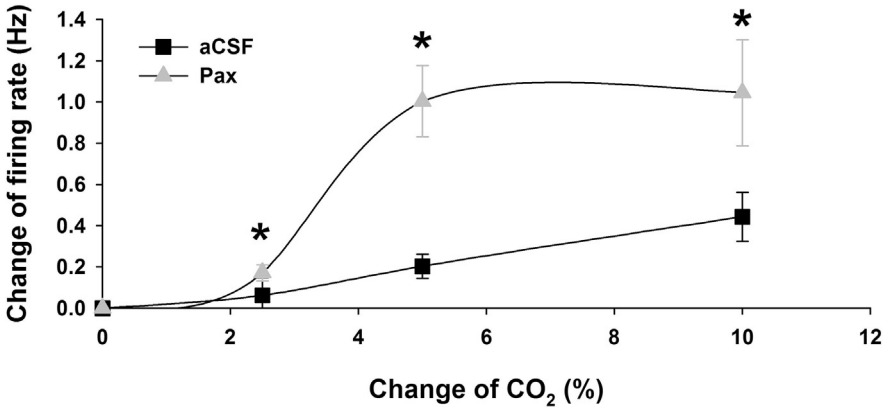

Fig. 6. The effect of paxilline on the CI and the increased firing rate of LC neurons in response to hypercapnia of 15%, 10% and 7.5% CO_2. When the ΔFR values for LC neurons, from rats older than P10, exposed to 7.5% CO_2, 10% CO_2 and 15% CO_2 with and without paxilline are plotted, it can be seen that paxilline induces a significant increase in firing rate at all levels of hypercapnic acidosis. The increased firing rate induced by paxilline was greatest for 15% (0.89 Hz; $n = 15$) and for 10% CO_2 (0.80 Hz; $n = 3$) but was much smaller, although significant, for 7.5% CO_2 (0.14 Hz; $n = 5$). $^{*}P < 0.05$. The zero in the "X" axis represents the normocapnic condition constituted by 5% CO_2 in the perfusion solution.

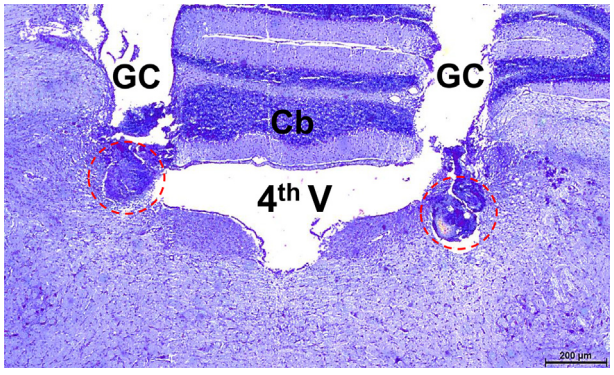

Fig. 7. Representative photomicrograph of a coronal section at the pons level illustrating the bilateral microinjection in the locus coeruleus (LC). This is an image of a coronal pons slice (15 µm) at the level of the LC. The slice was stained with Evan's blue, fixed in 10% formalin, embedded with paraffin and the microinjection sites were visualized using Nissl stain. The stained slice was visualized with a 10× objective. The sites of bilateral microinjection are outlined by the red dotted circles. 4thV: 4th ventricle; Cb: cerebellum; GC: paths of the guide cannulae. Scale bar = 200 µm.

increased internal Ca^{2+} was blocked by nifedipine, suggesting that it arises from Ca^{2+} entry through surface channels and not by release from internal stores (Fig. 2B). We did not quantify the hypercapnia-induced increase of Ca_i^{2+} in the soma of LC neurons but it appears to be small. However, it is likely that the increase of Ca^{2+} is much larger in a restricted space, probably submembranous or within nano-domains immediately surrounding Ca^{2+} channels, where it could affect ion channels within the surface membrane.

The role of Ca^{2+} in chemosensitivity of LC neurons

Although several types of H^+-sensitive K^+ currents and cation channels have been identified in LC neurons (Pineda and Aghajanian, 1997; Putnam, 2010; Cui et al., 2011; Li and Putnam, 2013) that increase LC neuron firing rate in response to hypercapnic acidosis, little is currently known about the role of Ca^{2+} in the chemosensitivity of the LC. The L-type Ca^{2+} channel blocker nifedipine decreased the chemosensitive firing rate response of LC neurons to hypercapnic acidosis from rats younger than P9 (Filosa and Putnam, 2003), suggesting that an increase in the L-type Ca^{2+} current, which would result in neuronal depolarization, contributes to the chemosensitive increase in firing rate in response to hypercapnic acidosis in LC neurons from rats younger than P9, which agrees with our current results showing that a chemosensitive increase in Ca^{2+} currents occurs during exposure to hypercapnic acidosis (Fig. 1D–F).

An increase in intracellular Ca^{2+} induced by hypercapnic acidosis means that numerous Ca^{2+}-dependent signaling pathways could be activated and thereby involved in the chemosensitive response of LC neurons. One such pathway that we studied here is the possibility that hypercapnia-induced elevation of intracellular Ca^{2+} activates BK channels and leads to hyperpolarization, and thus smaller increases of firing rate.

Activation of BK channels by hypercapnic acidosis-induced elevated Ca_i^{2+}: a chemosensitive brake

The accumulation of intracellular Ca^{2+} in response to hypercapnia in LC neuron somas raises the possibility that exposure to hypercapnic acidosis results in the activation of K_{Ca} channels. Sausbier et al. (2006) have shown with immunohistochemistry the marked presence of large-conductance K_{Ca} (BK) channels in the LC of mice. We were able to assess the activity of these channels using the BK channel inhibitor paxilline and a voltage-clamp protocol that yielded a paxilline difference current (Pax ΔI), which we attribute to BK channel activity (Fig. 3A–C). That these channels are Ca-activated K^+ channels is further indicated by the marked reduction of the peak Pax ΔI by nifedipine (Fig. 3E) or by loading the neuron with the Ca^{2+} chelator BAPTA (Fig. 3F). These findings show that while hypercapnic acidosis-induced depolarization may activate BK channels it is the increased intracellular Ca^{2+} induced by hypercapnia that is most responsible for activation of BK channels in LC neurons.

The activation of BK channels by hypercapnia-induced increased Ca^{2+} is also demonstrated by the effect of paxilline on the firing rate response of LC neurons to hypercapnic acidosis. LC neurons from neonatal rats older than P10 have a markedly increased firing rate response to hypercapnic acidosis in the presence compared to the absence of paxilline (Fig. 4A, B). These findings suggest that hypercapnic acidosis

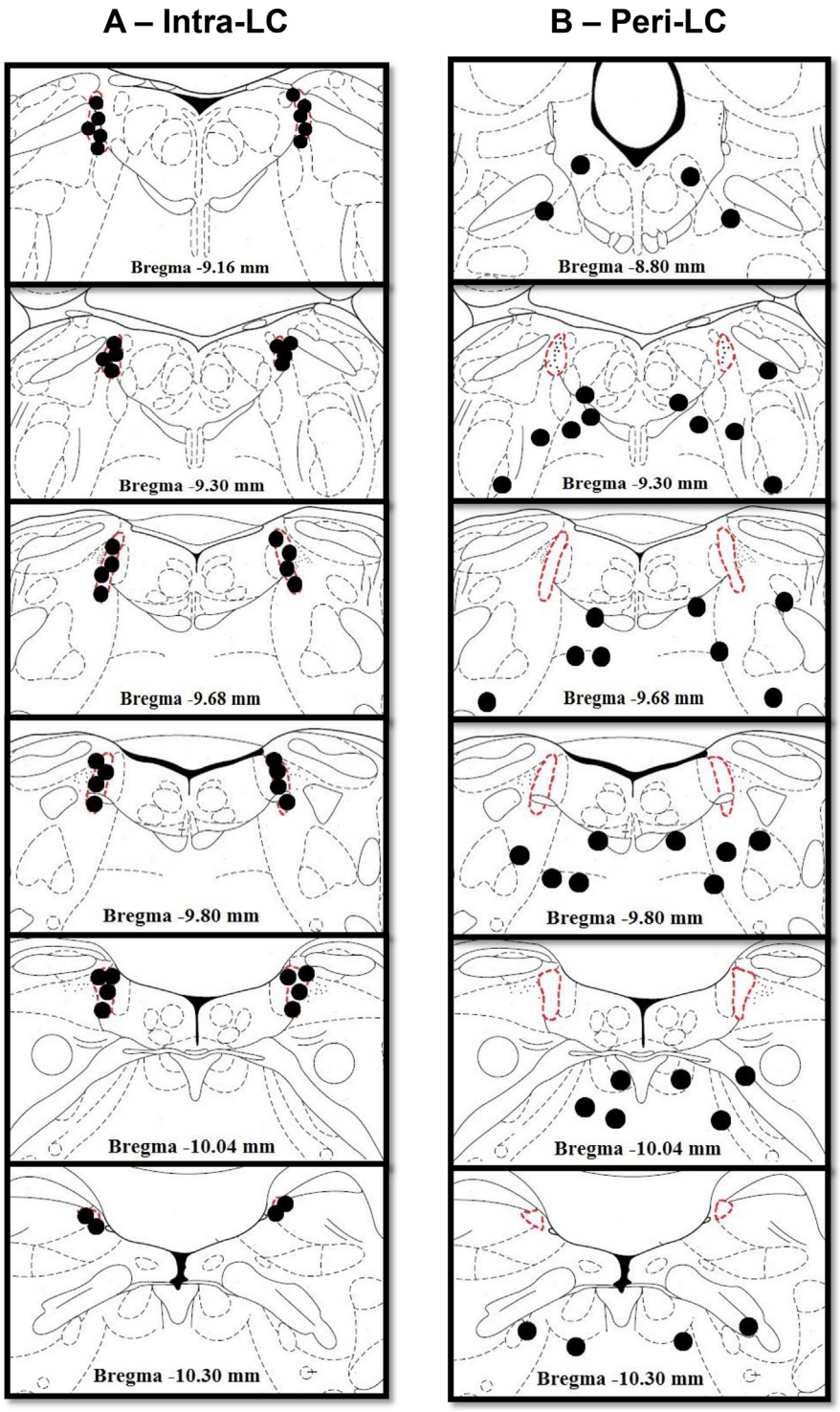

Fig. 8. Schematic representation of microinjection sites of intra and peri-LC throughout the extension of the locus coeruleus (LC). Representative diagrams of the site of microinjection adapted from Paxinos and Watson (1998) corresponding to the region where the LC is located showing microinjection sites (black circles) and the LC nucleus (outlined by dotted red lines). (A). Diagrams of transverse sections of the brainstem (−9.16 to −10.30 mm from bregma) showing distribution of all microinjection sites considered to be intra-LC (the sites are from 50 animals). (B). Diagrams of transverse sections of the brainstem (−8.80 to −10.30 mm from bregma) showing distribution of all microinjection sites considered to be peri-LC (the sites are from 7 animals).

activates BK channels by increasing Ca_i^{2+}, the BK channels hyperpolarize LC neurons and this hyperpolarization decreases the neuronal firing rate response to hypercapnic acidosis. When the BK channels are inhibited by paxilline, this hyperpolarizing effect is removed and the firing rate response to a hypercapnic acidotic challenge increases. Notably, when paxilline is applied to spontaneously firing LC neurons in control solutions (equilibrated with 5% CO_2), it has no effect on firing rate (Fig. 4A), indicating that BK channels are only active in the presence of hypercapnia. Some possible reasons why an activation of BK was not observed at resting membrane potential are: (1) There is not sufficient cytoplasmic calcium to activate BK, this suggests that intracellular Ca^{2+} is too low in resting LC neurons to activate BK channels; (2) The intracellular pipette solution we used did not contain calcium, which may reduce the calcium/BK effect on neuron activity; and the most plausible (3) BK channels do not play a role in the LC firing rate resting conditions, thus, paxilline perfusion does not change the resting membrane potential. Therefore, LC neurons BK channels seems to be specifically important during CO_2 exposure. In agreement, Sanchez-Padilla et al. (2014) showed that when L-type calcium channels were blocked by isradipine in the LC neurons, no change of firing rate was observed, suggesting that these channels are activated in specific situation, for example, under high CO_2 levels.

BK channels have been suggested to control firing rate in neurons under a variety of conditions. A point mutation in the human *KCNMA1* gene for the pore-forming subunit of the BK channel was identified in a familial form of epilepsy (Du et al., 2005). In LC neurons, burst firing rates, induced by injections of depolarizing current pulses, were found to be much greater in the presence of Ca^{2+} channel blockade (Sanchez-Padilla et al., 2014). These results are consistent with a hyperpolarizing function for BK channels that are sensitive to

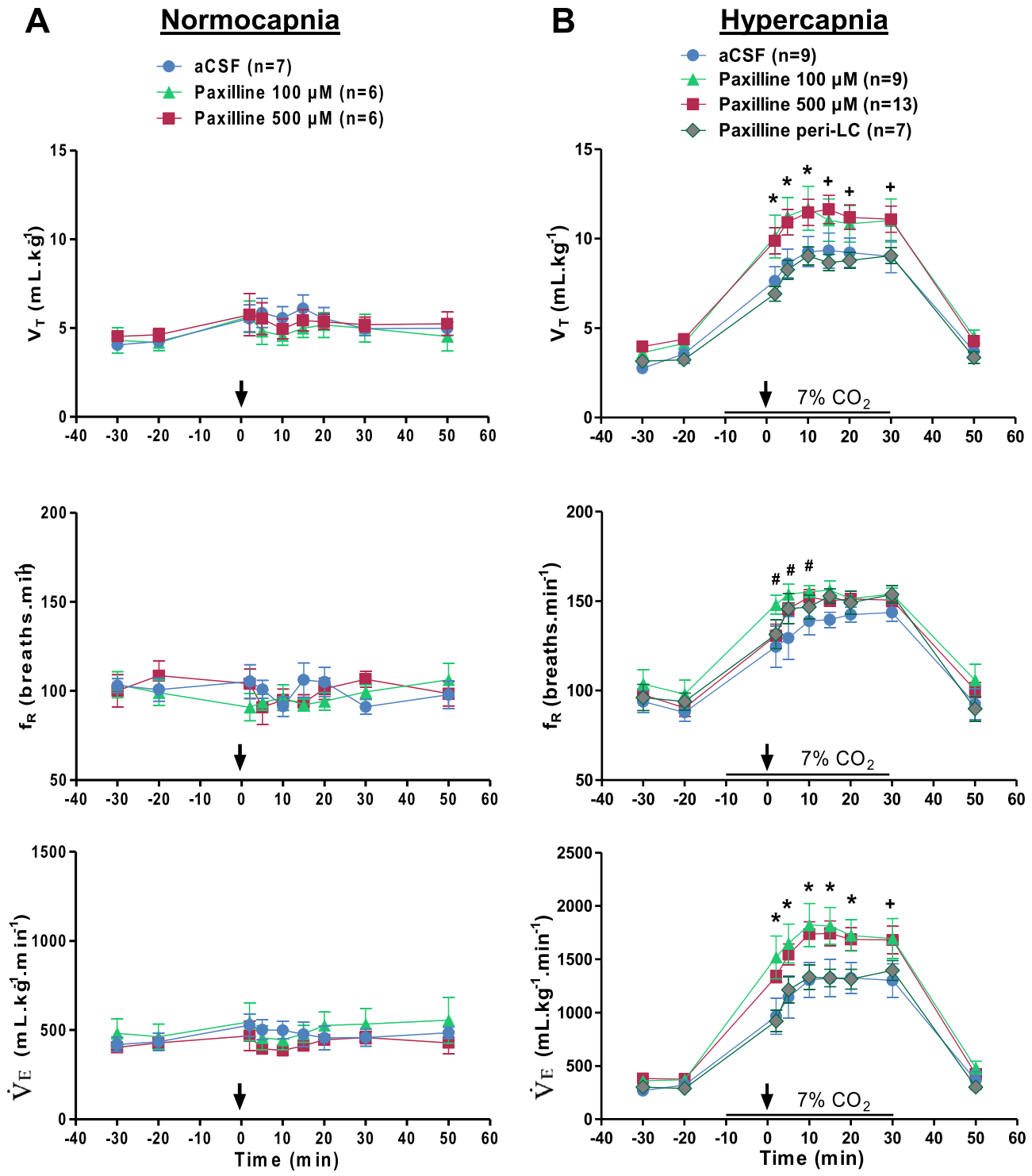

Fig. 9. Effect of bilateral injection of paxilline into the LC on ventilatory parameters in adult male rats breathing room air (normocapnia) or 7% CO_2 (hypercapnia). Effect of bilateral intra-LC vehicle (100 nL of aCSF) or paxilline (100 nL of either 100 µM or 500 µM paxilline) microinjections or bilateral peri-LC paxilline (100 nL of either 100 µM or 500 µM paxilline) microinjections in adult rats breathing room air (normocapnia – A) or 7% CO_2 (hypercapnia – B) on the tidal volume (V_T) (top panel), breathing frequency (f_R) (middle panel) and minute ventilation ($\dot{V}_E$) (bottom panel). Note that the injection of paxilline did not affect any of these variables under normocapnic conditions. For 7% CO_2 exposure, note that hypercapnia increases V_T and f_R in all microinjection groups, but the V_T was significantly bigger so when paxilline was microinjected ($P < 0.05$). The $\dot{V}_E$ was increased in all groups during high levels of CO_2, but paxilline microinjection groups showed a significantly larger hypercapnia-induced increase in $\dot{V}_E$ compared to the control and peri-LC injection group, largely driven by an increase in V_T ($P < 0.05$). All values are expressed as mean ± S.E.M. The arrow indicates when the microinjection occurred. The onset and duration of hypercapnia are marked on the graph. * Means significantly different between paxilline (100 µM and 500 µM) groups and control (vehicle and peri-LC injection) groups. + Means significantly different between paxilline 500 µM and control (vehicle and peri-LC injection) groups. # Means significantly different between paxilline 100 µM and vehicle group.

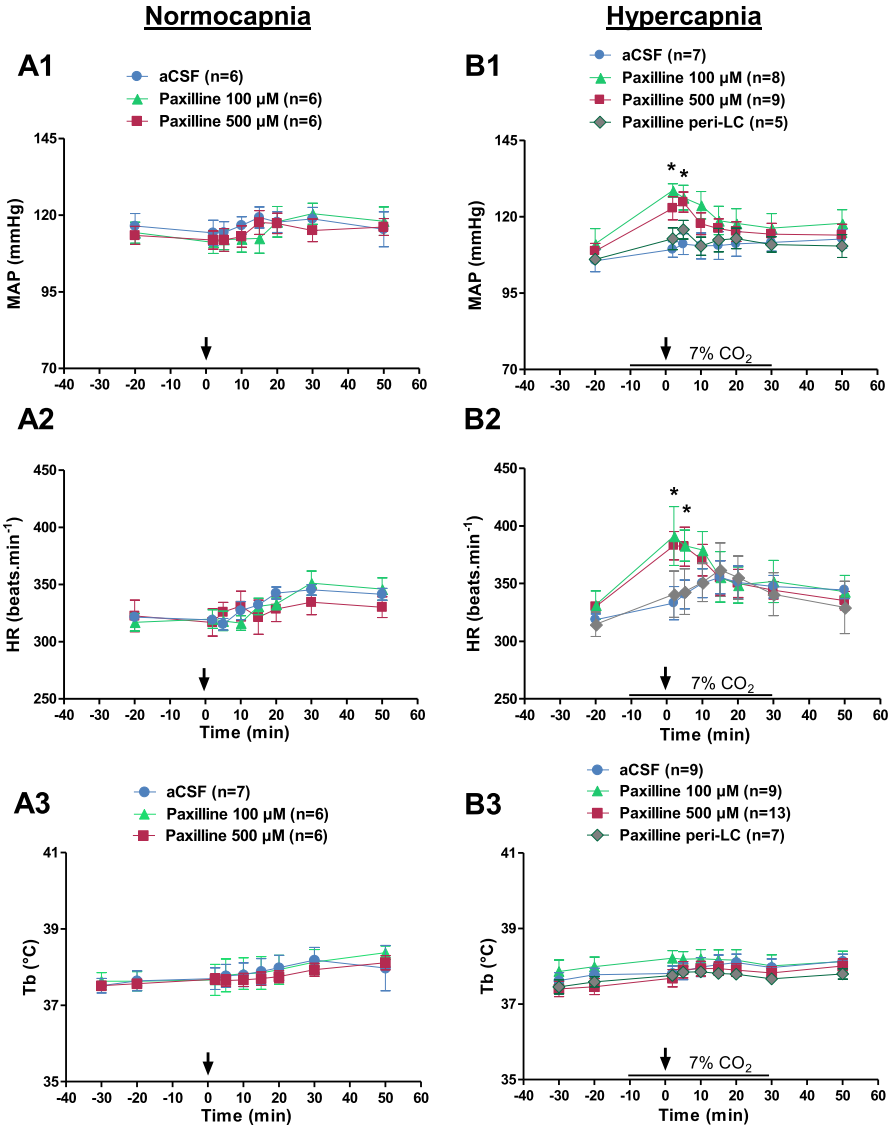

Fig. 10. Effect of bilateral microinjections of paxilline into the LC on cardiovascular parameters and body temperature in adult male rats breathing room air (normocapnia) or 7% CO_2 (hypercapnia). Effect of bilateral intra-LC vehicle (100 nL of aCSF) or paxilline (100 nL of either 100 μM or 500 μM paxilline) microinjections or bilateral peri-LC paxilline (100 nL of either 100 μM or 500 μM paxilline) microinjections on mean arterial pressure (A1, B1; MAP), heart rate (A2, B2; HR) and body temperature (A3, B3; Tb) in adult male rats under normocapnic (room air; A) or hypercapnic (7% CO_2; B) conditions. In rats breathing room air paxilline microinjection into the LC had no effect on MAP (A1), HR (A2) or Tb (A3). During hypercapnic exposure the MAP of the paxilline (100 μM or 500 μM) groups was significantly higher ($P < 0.05$) compared with the vehicle and peri-LC group (B1). HR was also significantly higher in the paxilline-treated rats (100 μM or 500 μM) compared to vehicle and peri-LC injection ($P < 0.05$) in the presence of hypercapnia (B2). Paxilline microinjections into the LC did not affect Tb in rats breathing hypercapnia (B3). An arrow indicates the time of microinjection. Values are expressed as mean ± S.E.M. The onset and duration of hypercapnia are marked on each graph. * Means significantly different between paxilline-treated (100 μM and 500 μM) rats and control (vehicle and peri-LC injection) group.

Ca^{2+} influx via voltage-activated channels. Lowering Ca_i^{2+} levels in LC neurons by loading with EGTA was also found to increase the spontaneous firing rate, as would be expected with the decreased activity of a hyperpolarizing K_{Ca} channel (Aghajanian et al., 1983). Thus, it seems likely that the role for BK channels in LC neurons is to limit the increase in firing rate via a negative-feedback mechanism through increases in Ca_i^{2+} (Aghajanian et al., 1983; Fakler and Adelman, 2008). Additionally, we have previously demonstrated that the activation of L-type Ca_2^+ channels by hypercapnia in LC neurons is mediated by the presence of a HCO_3^--dependent pathway, involving soluble adenylate cyclase and protein kinase A, and more details for the cell brake phenomenon mechanism can be found on Imber et al. (2014).

Apamin-sensitive, small conductance (S_k) K_{Ca} channels have also been identified in LC neurons (Williams et al., 1984; Osmanovic and Shefner, 1993). Unlike BK channels, S_k channels have no voltage dependence and are gated solely by Ca_i^{2+} (Fakler and Adelman, 2008). Thus, S_k channels in LC neurons should also be activated by the chemosensitive increase in Ca_i^{2+} and may contribute to the braking mechanism along with BK channels (Fig. 3A).

Development of the chemosensitive brake in LC neurons

Postnatal developmental changes of Ca^{2+} channel activity has been reported in many regions of the CNS (Iwasaki et al., 2000). We previously studied TTX-insensitive spikes and oscillations in LC neurons which arise from the activity of L-type Ca^{2+} channels (Imber and Putnam, 2012). We found that the frequency of these spikes and oscillations increased during the postnatal period from P3 to P16, suggesting that L-type Ca^{2+} currents increase during postnatal development. In the current study, we show that Ca^{2+} channel current density significantly increases in LC neurons over postnatal ages P3–P14 (Fig. 1B, inset). As expected, it appears that intracellular Ca^{2+} (based on changes in R_{fl}) also increases in parallel with the increase in Ca^{2+} channel density, both under normocapnic conditions and under hypercapnia (Fig. 2B).

Based on the above findings, it would be expected that BK activity should also increase with postnatal development as there will be a higher concentration of intracellular Ca^{2+} in LC neurons from older neonates. In fact, we found a significantly increased BK channel current density in LC neurons from older neonatal rats (P13–15) compared to LC neurons from younger neonatal rats (P3–4). These current density values suggest that BK channels

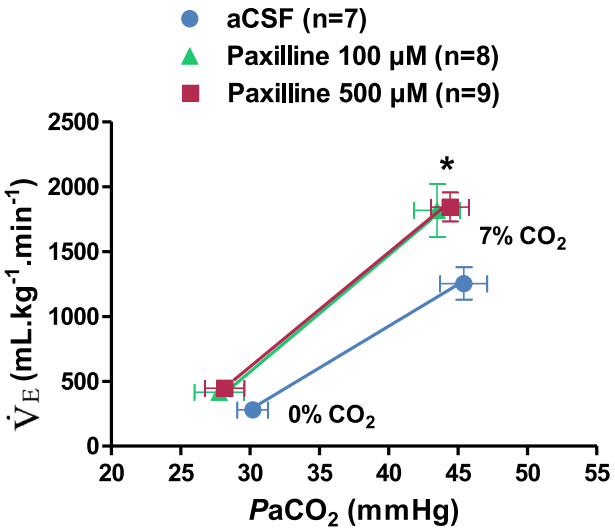

Fig. 11. Effect of bilateral microinjections of paxilline into the LC on CO_2 sensitivity. Effect of bilateral intra-LC vehicle (100 nL of aCSF) or paxilline (100 nL of either 100 μM or 500 μM paxilline) microinjections on CO_2 sensitivity (relationship between $\dot{V}_E$ and P_{aCO2}). In the paxilline-treated rats (100 μM or 500 μM) the sensitivity curves presented a significant higher slopes than the vehicle curve ($P < 0.05$). Values are expressed as mean ± S.E.M.

undergo postnatal development in LC neurons, increasing during the first two postnatal weeks.

That both Ca^{2+} channels and BK channels undergo development in LC neurons during the first two postnatal weeks suggests that the braking phenomenon, resulting from activation of BK channels, should similarly undergo development, becoming more prominent in LC neurons with increasing postnatal age. This is shown in Fig. 4, where the effect of inhibition of BK channels on the firing rate response to hypercapnic acidosis is very small in LC neurons from rats younger than P10, but it is quite prominent in LC neurons from rats older than P10 (Fig. 4B). The decreased firing rate in response to hypercapnic acidosis due to activation of the BK channel should result in a decreased chemosensitivity index in LC neurons from rats with increasing neonatal age. This has been previously reported (Gargaglioni et al., 2010) and we confirmed it in the present study (Fig. 5A). Our findings strongly suggest that this decrease in CI is due largely to the development of the brake and specifically, the increased BK channel density with increasing neonatal age. This is supported by the strong correlation between BK channel current density and CI in LC neurons from neonatal rats of different age (Fig. 5B). Thus, the brake proposed here appears to be a major determinant of the magnitude of the chemosensitive firing rate response of LC neurons to hypercapnic acidosis during early development. The unusual developmental decrease in chemosensitivity in LC neurons suggests that LC neurons play a role in the control of breathing early in development but this role may shift to more of an alarm response to elevated levels of CO_2 in older neonates.

Our data strongly suggest that the decrease in the chemosensitive response in LC neurons from older neonates is due to the development of the brake. First, the fall of the firing rate response to hypercapnic acidosis shows a strong negative correlation to the development of the BK current density (Fig. 5B) and inhibition of the BK current in older neonates nearly completely restores the large firing rate response to hypercapnic acidosis seen in young neonates (Fig. 6) although this is not true at lower levels of hypercapnic challenges, suggesting other factors may also be involved in the decrease of CI with age in LC neurons from neonatal rat pups. This role for Ca^{2+} and BK channels in the chemosensitive neurons of the LC represents a novel approach to the magnitude of the response to hypercapnic acidosis in chemosensitive neurons.

The magnitude of the brake in response to different levels of hypercapnic acidosis

The magnitude of the braking effect (as measured by the increase in LC neuron firing rate in response to hypercapnic acidosis in the presence vs. the absence of paxilline) is large when the hypercapnic acidotic stimulus is 15% CO_2 (Fig. 6). This is a very high level of CO_2. A lower level of hypercapnic acidosis (10% CO_2), which is often used to study the induction of panic reactions (Ziemann et al., 2009) also causes a large braking effect. However, a relatively low hypercapnic acidotic stimulus (7.5% CO_2; control CO_2 is 5%) causes a significant but small braking effect in LC neurons (Fig. 6). These findings suggest that the braking phenomenon in LC neurons may play a role in responses to higher levels of hypercapnic acidosis, such as with panic disorders, but it is unclear whether this braking phenomenon plays any role in the control of breathing, which usually involves much smaller levels of hypercapnic acidosis.

Effect of paxilline on the hypercapnic ventilatory response of adult rats

We directly tested whether the braking phenomenon in LC neurons could play a role in the control of breathing. Inhibiting the brake with bilateral injections of paxilline into the LC had no effect on ventilation in rats breathing room air (Fig. 9A) but significantly increased the hypercapnic ventilatory response (by about 30%) to inspired CO_2 of 7% (Fig. 9B). This increase was largely mediated by an increase in the tidal volume response to hypercapnia, although initially an increase in respiratory frequency was also seen (Fig. 9B). This mechanism of response shows to be particular, but not exclusive, to the LC since the injections surrounding the nucleus did not cause any change in these variables (Fig. 9B). The LC has previously been shown to be capable of altering both the respiratory frequency and the tidal volume in response to hypercapnia. Lesioning of LC noradrenergic neurons in adult rats decreased the hypercapnic ventilatory response to 7% CO_2 by about 64% and this was largely due to a decrease in tidal volume (Biancardi et al., 2008). However, inhibition of gap junctions in LC neurons by injection of carbenoxolone into the LC of adult rats decreased the hypercapnic ventilatory response to 7% CO_2 by about 25% but this decrease was largely

mediated by a reduced response of respiratory frequency (Patrone et al., 2014). Interestingly, neither lesioning of LC noradrenergic neurons nor the injection of carbenoxolone (up to 1 mM) into the LC had any effect on the mean arterial pressure or the heart rate, either in normocapnia or in 7% CO_2 (Biancardi et al., 2008; Patrone et al., 2014), although the injection of 3 mM carbenoxolone significantly lowered the heart rate under hypercapnic (7% CO_2) conditions (Patrone et al., 2014). These studies show that the LC does not appear to play a major role in cardiovascular control under conditions that reduces the activity of LC neurons. However, LC lesion with substance P-saporin conjugate caused an increase in heart rate increased after CO_2 challenge suggesting that neurokinin-1 expressing neurons in the LC are involved in the regulation of heart rate during CO_2 exposure (De Carvalho et al., 2010). In the present study, inhibition of BK channels by paxilline and thereby inhibition of the brake in the LC resulted in transient increases of both mean arterial pressure and heart rate in the presence of 7% CO_2 (Fig. 10B1, B2). These findings suggest that inhibiting the brake in LC neurons can affect the cardiovascular response as well as the respiratory response to hypercapnia.

It is noteworthy that the effects of paxilline on the firing rate of individual LC neurons parallels the effects of paxilline injection into the LC on ventilatory responses. Paxilline has no effect on the basal firing rate of LC neurons in normocapnia nor does LC injection have any effect on ventilation under normocapnic conditions. In contrast, paxilline both increases the firing rate of LC neurons to hypercapnic acidosis and increases the hypercapnic ventilatory response.

SUMMARY AND SIGNIFICANCE

This study presents evidence for a new pathway for the regulation of the response of chemosensitive neurons to hypercapnic acidosis, a braking pathway. Several studies of chemosensitive glomus cells (Kim, 2013) and medullary neurons in culture (Wellner-Kienitz et al., 1998) have shown that inhibition of Ca^{2+}-activated K^+ channels results in an increased response to hypercapnic acidosis. However, these studies are fundamentally different than the current study. In these studies, the inhibition of K_{Ca} channels by hypercapnic acidosis is presumed to be due to acidification. For these cells to have an increased response to hypercapnic acidosis, the K_{Ca}-channels would have to be active in the cells under normocapnic conditions. Upon exposure to hypercapnic acidotic conditions inhibition of the K_{Ca} channels results in cellular depolarization and activation. As such, the K_{Ca} channels are viewed as just another outwardly-conducting K^+ channel whose inhibition by acidosis leads to cellular activation. Our model is fundamentally different. The BK channels in LC neurons are not active under normocapnic conditions and are activated by hypercapnia in a HCO_3^- – dependent fashion (Imber et al., 2014). This activation results in an enhanced hyperpolarizing effect that reduces the neuronal response to hypercapnic acidosis. The BK channels are not apparently inhibited by acidosis, even at high levels of CO_2. Thus, this brake is normally active in the presence of hypercapnic acidosis and requires some inhibitory agent to remove the braking effect. Factors that would alter this pathway could result in altered respiratory drive, as demonstrated in this study by injection of paxilline into the LC of adult rats. Thus, our study suggests that respiratory drive can be altered either by altering the acid-sensitive channels that lead to chemosensitive neuronal activation (accelerator pathway) or by altering the activation of BK channels that leads to decreased chemosensitive neuronal activity (braking pathway).

There is an interesting corollary to this idea that the magnitude of the chemosensitive response of LC neurons reflects a balance between hypercapnia-induced activation of accelerator pathways vs. braking pathways. One can imagine under certain circumstances that the braking pathway could be as powerful as the accelerator pathways. Such a neuron would appear to be nonchemosensitive. Further, if the braking pathway is the predominant pathway, the firing rate of such neurons might decrease in response to hypercapnic acidosis. Such neurons would be inhibited by hypercapnic acidosis, as has been observed in neurons from several chemosensitive areas (Putnam et al., 2004). Thus, highly active braking pathways could provide a previously unknown mechanistic basis for hypercapnia-inhibited neurons.

The braking pathway appears to be minimally active, if at all, in LC neurons from newly born rats, but develops over the first two weeks of life, resulting in a marked decrease in the chemosensitivity of LC neurons with development. Our findings that paxilline injection into the LC of adult rats increases the hypercapnic ventilatory response indicates that this braking pathway, once developed, is retained and is active into adulthood.

The implications of this chemosensitive braking pathway are significant to studies on human pathology. In cases of obstructive sleep apnea (OSA), multiple clinical studies have documented an association between OSA and an increase in the loop gain, or the ratio of ventilatory increase to a disturbance that initiates ventilation (Verbraecken et al., 1995; Younes et al., 2001; Wang et al., 2007). In other words, an increase in respiratory gain was associated with the onset of irregular breathing, and medications designed to decrease loop gain were demonstrated to be effective treatments (Kiwull-Schöne et al., 2008). Other studies have more directly associated an increase in the ventilatory sensitivity to CO_2 with respiratory pathology (Chapman et al., 1988; Wang et al., 2007). Thus, alterations in the development of a CO_2-sensitive braking pathway designed to limit the chemosensitive gain may have implications for respiratory disease. More specific to neurons of the LC is the profound body of evidence linking the pathology of panic disorder to respiratory abnormalities, including an enhanced sensitivity to CO_2 (Lousberg et al., 1988; Papp et al., 1993; Stein et al., 1995; Abelson et al., 2001; Nardi et al., 2009). Since the noradrenergic neurons of the LC are (1) already implicated by electrophysiological and immunohistochemical

studies with the fear response of the amygdala, and (2) are chemosensitive with over 80% of LC neurons sensitive to CO_2, it seems likely that the LC contributes to such a CO_2-induced fear response (Filosa et al., 2002; Buffalari and Grace, 2007). Accordingly, abnormalities in a chemosensitive braking pathway in LC neurons may have direct implications for the sensitivity to CO_2 of panic disorder patients and targeting the braking pathway may represent a novel approach for treatment of this disorder.

ACKNOWLEDGMENTS AND AUTHOR CONTRIBUTIONS

Dedicated to the memory of Robert W. Putnam, inspiring mentor and dear friend. ANI, KYL, LGAP, LHG and RWP conceived and designed the experiments and ANI, KYL and LGAP performed the experiments. KYL designed and performed some of the experiments with 7.5% and 10% CO_2. ANI, KYL, LGAP, LHG and RWP wrote a draft of and edited the manuscript. All experiments were done in the laboratory of RWP except for the microinjection and plethysmography experiments which were done in the laboratory of LHG. All authors approved the final version of this manuscript.

CONFLICT OF INTEREST

The authors declare no competing interests.

This work was supported by National Heart, Lung, and Blood Institute (NHLBI, USA) Grant R01 HL-56683 (to RWP), an American Heart Association Great Rivers Affiliate (USA) Pre-doctoral Fellowship (to ANI), and a Research Challenge Augmentation Grant from Wright State University – USA (to RWP). This work was also supported by Brazilian public funding from *Fundação de Amparo à Pesquisa do Estado de São Paulo* (FAPESP, Brazil) (grant: 2016/24577-3 to LHG and grant: 2010/06210-9 to LGAP), the *Conselho Nacional de Desenvolvimento Cientifico e Tecnológico* (CNPq) and *INCT-Fisiologia Comparada*.

REFERENCES

Abelson JL, Weg JG, Nesse RM, Curtis GC (2001) Persistent respiratory irregularity in patients with panic disorder. Biol Psychiatry 49:588–595.

Aghajanian GK, Vandermaelen CP, Andrade R (1983) Intracellular studies on the role of calcium in regulating the activity and reactivity of locus coeruleus neurons *in vivo*. Brain Res 273:237–243.

Bailey JE, Argyropoulos SV, Lightman SL, Nutt DJ (2003) Does the brain noradrenaline network mediate the effects of the CO_2 challenge? J Psychopharmacol 17:252–259.

Bartlett D, Tenney SM (1970) Control of breathing in experimental anemia. Respir Physiol 10:384–395.

Bayliss DA, Talley EM, Sirois JE, Lei Q (2001) TASK-1 is a highly modulated pH-sensitive 'leak' K^+ channel expressed in brainstem respiratory neurons. Respir Physiol 129:159–174.

Biancardi V, Bicego KC, Almeida MC, Gargaglioni LH (2008) Locus coeruleus noradrenergic neurons and CO_2 drive to breathing. Pflügers Arch 455:1119–1128.

Buffalari DM, Grace AA (2007) Noradrenergic modulation of basolateral amygdala neuronal activity: opposing influences of alpha-2 and beta receptor activation. J Neurosci 27:12358–12366.

Chapman KR, Bruce EN, Gothe B, Cherniack NS (1988) Possible mechanisms of periodic breathing during sleep. J Appl Physiol 64:1000–1008.

Chieng B, Bekkers JM (1999) GABA(B), opiod and alpha2 receptor inhibition of calcium channels in acutely-dissociated locus coeruleus neurons. Br J Pharmacol 127:1533–1538.

Conrad SC, Nichols NL, Ritucci NA, Dean JB, Putnam RW (2009) Development of chemosensitivity in neurons from the nucleus tractus solitarii (NTS) of neonatal rats. Respir Physiol Neurobiol 166:4–12.

Cui N, Zhang X, Tadepalli JS, Yu L, Gai H, Petit J, Pamulapati RT, Jin X, Jiang C (2011) Involvement of TRP channels in the CO_2 chemosensitivity of locus coeruleus neurons. J Neurophysiol 105:2791–2801.

De Carvalho D, Bicego KC, De Castro OW, Da Siva GS, Garcia-Cairasco N, Gargaglioni LH (2010) Role of neurokinin-1 expressing neurons in the locus coeruleus on ventilatory and cardiovascular responses to hypercapnia. Respir Physiol Neurobiol 172:24–31.

Dean JB, Lawing WL, Millhorn DE (1989) CO_2 decreases membrane conductance and depolarizes neurons in the nucleus tractus solitarii. Exp Brain Res 76:656–661.

Denton JS, McCann FV, Leiter JC (2007) CO_2 chemosensitivity in *Helix aspersa*: three potassium currents mediate pH-sensitive neuronal spike timing. Am J Physiol Cell Physiol 292: C292–C304.

Du W, Bautista JF, Yang H, Diez-Sampedro A, You SA, Wang L, Kotagal P, Luders HO, Shi J, Cui J, Richerson GB, Wang QK (2005) Calcium-sensitive potassium channelopathy in human epilepsy and paroxysmal movement disorder. Nat Genet 37:733–738.

Fakler B, Adelman JP (2008) Control of K_{Ca} channels by calcium nano/microdomains. Neuron 59:873–881.

Filosa JA, Dean JB, Putnam RW (2002) Role of intracellular and extracellular pH in the chemosensitive response of rat locus coeruleus neurones. J Physiol 541:493–509.

Filosa JA, Putnam RW (2003) Multiple targets of chemosensitive signaling in locus coeruleus neurons: role of K^+ and Ca^{2+} channels. Am J Physiol Cell Physiol 284:C145–C155.

Gargaglioni LH, Hartzler LK, Putnam RW (2010) The locus coeruleus and central chemosensitivity. Respir Physiol Neurobiol 173:264–273.

Golowasch J, Thomas G, Taylor AL, Patel A, Pineda A, Khalil C, Nadim F (2009) Membrane capacitance measurements revisited: dependence of capacitance value on measurement method in nonisopotential neurons. J Neurophysiol 102:2161–2175.

Gorman JM, Browne ST, Papp LA, Martinez J, Welkowitz L, Coplan JD, Goetz RR, Kent J, Klein DF (1997) Effect of antipanic treatment on response to carbon dioxide. Biol Psychiatry 42:982–991.

Hodges MR, Richerson GB (2010) Medullary serotonin neurons and their roles in central respiratory chemoreception. Respir Physiol Neurobiol 173:256–263.

Imber AN, Putnam RW (2012) Postnatal development and activation of L-type Ca^{2+} currents in locus coeruleus neurons: implications for a role for Ca^{2+} in central chemosensitivity. J Appl Physiol 112:1715–1726.

Imber AN, Santin JM, Graham CD, Putnam RW (2014) A HCO_3^- - dependent mechanism involving soluble adenylyl cyclase for the activation of Ca^{2+} currents in locus coeruleus neurons. Biochim Biophys Acta 1842:2569–2578.

Iwasaki S, Momiyama A, Uchitel OD, Takahashi T (2000) Developmental changes in calcium channel types mediating central synaptic transmission. J Neurosci 20:59–65.

Kim D (2013) K^+ channels in O_2 sensing and postnatal development of carotid body glomus cell response to hypoxia. Respir Physiol Neurobiol 185:44–56.

Kiwull-Schöne H, Teppema L, Wiemann M, Kalhoff H, Kiwull P (2008) Pharmacological impact on loop gain properties to prevent irregular breathing. J Physiol Pharmacol 59:37–45.

Kunert-Keil C, Bisping F, Krüger J, Brinkmeier H (2006) Tissue-specific expression of TRP channel genes in the mouse and its variation in three different mouse strains. BMC Genomics 7:159.
Li K-Y, Putnam RW (2013) Transient outwardly rectifying A currents are involved in the firing rate response to altered CO_2 in chemosensitive locus coeruleus neurons from neonatal rats. Am J Physiol Regul Integr Comp Physiol 305:R780–R792.
Lipscombe D, Helton TD, Xu W (2004) L-type calcium channels: the low down. J Neurophysiol 92:2633–2641.
Lousberg H, Grie E, Van den Hout MA (1988) Carbon dioxide chemosensitivity in panic disorder. Acta Psychiatr Scand 77:214–218.
Marcantoni A, Vandael DH, Mahapatra S, Carabelli V, Sinnegger-Brauns MJ, Striessnig J, Carbone E (2010) Loss of Cav1.3 channels reveals the critical role of L-type and BK channel coupling in pacemaking mouse adrenal chromaffin cells. J Neurosci 30:491–504.
Mulkey DK, Stornetta RL, Weston MC, Simmons JR, Parker A, Bayliss DA, Guyenet PG (2004) Respiratory control by ventral surface chemoreceptor neurons in rats. Nat Neurosci 7:1360–1369.
Nardi AE, Freire RC, Zin WA (2009) Panic disorder and control of breathing. Respir Physiol Neurobiol 167:133–143.
Nichols NL, Mulkey DK, Wilkinson KA, Powell FL, Dean JB, Putnam RW (2009) Characterization of the chemosensitive response of individual solitary complex neurons from adult rats. Am J Physiol Regul Integr Comp Physiol 296:763–773.
Osmanovic SS, Shefner SA (1993) Calcium-activated hyperpolarizations in rat locus coeruleus neurones in vitro. J Physiol 469:89–109.
Papp LA, Klein DF, Gorman JM (1993) Carbon dioxide hypersensitivity, hyperventilation, and panic disorder. Am J Psychiatry 150:1149–1157.
Patrone LGA, Bicego KC, Hartzler LK, Putnam RW, Gargaglioni LH (2014) Cardiorespiratory effects of gap junction blockade in the locus coeruleus in unanesthetized adult rats. Respir Physiol Neurobiol 190:86–95.
Paxinos G, Watson C (2005) The rat brain in stereotaxic coordinates. 5th Edition. Boston: Elsevier Academic Press.
Pineda J, Aghajanian GK (1997) Carbon dioxide regulates the tonic activity of locus coeruleus neurons by modulating a proton- and polyamine-sensitive inward rectifier potassium current. Neuroscience 77:723–743.
Pols H, Lousberg H, Zandbergen J, Griez E (1993) Panic disorder patients show decrease in ventilatory response to CO_2 after clomipramine treatment. Psychiatry Res 47:295–296.
Putnam RW (2010) CO_2 chemoreception in cardiorespiratory control. J Appl Physiol 108:1796–1802.
Putnam RW, Filosa JA, Ritucci NA (2004) Cellular mechanisms involved in CO_2 and acid signaling in chemosensitive neurons. Am J Physiol Cell Physiol 287:C1493–C1526.
Richerson GB (1995) Response to CO_2 of neurons in the rostral ventral medulla in vitro. J Neurophysiol 73:933–944.
Ritucci NA, Erlichman JS, Leiter JC, Putnam RW (2005) Response of membrane potential and intracellular pH to hypercapnia in neurons and astrocytes from rat retrotrapezoid nucleus. Am J Physiol Regul Integr Comp Physiol 289:R851–R861.
Ritucci NA, Dean JB, Putnam RW (2005) Somatic vs. dendritic responses to hypercapnia in chemosensitive locus coeruleus neurons from neonatal rats. Am J Physiol Cell Physiol 289: C1094–C1104.
Sanchez-Padilla J, Guzman JN, Ilijic E, Kondapalli J, Galtieri DJ, Yang B, Schieber S, Oertel W, Wokosin D, Schumacker PT, Surmeier DJ (2014) Mitochondrial oxidant stress in locus coeruleus is regulated by activity and nitric oxide synthase. Nat Neurosci 17:832–842.
Sausbier U, Sausbier M, Sailer CA, Arntz C, Knaus H, Neuhuber W, Ruth P (2006) Ca^{2+}-activated K^+ channels of the BK-type in the mouse brain. Histochem Cell Biol 125:725–741.
Shah MJ, Meis S, Munsch T, Pape H (2001) Modulation by extracellular pH of low- and high-voltage-activated calcium currents of rat thalamic relay neurons. J Neurophysiol 85:1051–1058.
Stein MB, Millar TW, Larsen DK, Kryger MH (1995) Irregular breathing during sleep in patients with panic disorder. Am J Psychiatry 152:1168–1173.
Suwabe T, Mistretta CM, Krull C, Bradley RM (2011) Pre- and postnatal differences in membrane, action potential, and ion channel properties of rostral nucleus of the solitary tract neurons. J Neurophysiol 106(5):2709–2719.
Tombaugh GC, Somjen GG (1997) Differential sensitivity to intracellular pH among high- and low-threshold Ca^{2+} currents in isolated rat CA1 neurons. J Neurophysiol 77:639–653.
Verbraecken J, De Backer W, Willemen M, De Cock W, Wittesaele W, Van de H (1995) Chronic CO_2 drive in patients with obstructive sleep apnea and effect of CPAP. Respir Physiol 101:279–287.
Wang D, Grunstein RR, Teichtahl H (2007) Association between ventilatory response to hypercapnia and obstructive sleep apnea-hypopnea index in asymptomatic subjects. Sleep Breath 11:103–108.
Wang W, Pizzonia JH, Richerson GB (1998) Chemosensitivity of rat medullary raphe neurones in primary tissue culture. J Physiol 511:433–450.
Wang W, Richerson GB (1999) Development of chemosensitivity of rat medullary raphe neurons. Neuroscience 90:1001–1011.
Warren RA, Jones EG (1997) Maturation of neuronal form and function in a mouse thalamo-cortical circuit. J Neurosci 17 (1):277–295.
Wellner-Kienitz MC, Shams H, Scheid P (1998) Contribution of Ca^{2+}-activated K^+ channels to central chemosensitivity in cultivated neurons of fetal rat medulla. J Neurophysiol 79:2885–2894.
Williams JT, North RA, Shefner SA, Nishi S, Egan TM (1984) Membrane properties of rat locus coeruleus neurons. Neuroscience 13:137–156.
Williams RH, Jensen LT, Verkhratsky A, Fugger L, Burdakov D (2007) Control of hypothalamic orexin neurons by acid and CO_2. Proc Natl Acad Sci USA 104:10685–10690.
Younes M, Ostrowski M, Thompson W, Leslie C, Shewchuk W (2001) Chemical control stability in patients with obstructive sleep apnea. Am J Respir Crit Care Med 163:1181–1190.
Ziemann AE, Allen JE, Dahdaleh NS, Drebot II, Coryell MW, Wunsch AM, Lynch CM, Faraci FM, Howard MA, Welsh MJ, Wemmie JA (2009) The amygdala is a chemosensor that detects carbon dioxide and acidosis to elicit fear behavior. Cell 139:1012–1021.

(Received 6 November 2017, Accepted 13 March 2018)
(Available online 24 April 2018)